Printable metal oxide nanostructures based chemiresistive non-biological analyte sensors

NANO EXPRESS

TOPICAL REVIEW

Printable metal oxide nanostructures based chemiresistive non-biological analyte sensors

Amit Kumar[1], **Sang Sub Kim**[2], **Hyoun Woo Kim**[3] **and Mahesh Kumar**[1,4]

[1] Department of Electrical Engineering, Indian Institute of Technology Jodhpur, Jodhpur 342030, India
[2] Department of Materials Science and Engineering, Inha University, Incheon 22212, Republic of Korea
[3] Division of Materials Science and Engineering, Hanyang University, Seoul 04763, Republic of Korea
[4] Department of Cybernetics, Nanotechnology and Data Processing, Faculty of Automatic Control, Electronics and Computer Science, Silesian University of Technology, Akademicka16, 44-100 Gliwice, Poland

E-mail: sangsub@inha.ac.kr, hyounwoo@hanyang.ac.kr and mkumar@iitj.ac.in

Keywords: semiconductor metal oxides, chemiresistive sensors, printable electronics, non-biological analyte

OPEN ACCESS

RECEIVED
17 May 2023

REVISED
23 September 2023

ACCEPTED FOR PUBLICATION
23 October 2023

PUBLISHED
7 November 2023

Abstract

Non-biological analyte sensing refers to the ability to detect and quantify various chemical and physical parameters present in the environment or biological samples that are not directly associated with biological entities such as cells, tissues, or organisms. The field of non-biological analyte sensing has its roots in the early detection of any analytes, and over the years, it has expanded to include a wide range of applications such as environmental monitoring, food safety, and medical diagnostics. This perspective focuses on the current status, challenges and future prospects of metal oxide nanostructures-based non-biological analyte sensors. In this context, the present review aims to delve into the intricate mechanisms, fabrication techniques, and applications of printable chemical sensors for non-biological analytes. Through a comprehensive exploration of the scientific advancements and technological breakthroughs in this domain, this review seeks to provide a comprehensive understanding of the evolving landscape of printable chemical sensors and their pivotal role in modern analytical endeavours.

1. Introduction

Printable chemical sensors have emerged as innovative tools in the field of analytical chemistry, offering versatile and adaptable means of detecting and quantifying non-biological analytes. Harnessing the principles of materials science and nanotechnology, printable chemical sensors are fabricated using advanced printable materials such as conductive polymers [1], metal oxides (MOs) [2], carbon nanotubes [3], graphene [4], and functionalized nanoparticles. These materials offer the advantage of being easily deposited onto various substrates, including flexible and low-cost surfaces, through techniques like inkjet printing, screen printing, and aerosol jet printing [5]. Such approaches facilitate the creation of sensor arrays and customized designs, enabling tailored sensor platforms for specific non-biological analytes. Among all the material MOs based sensors are among the most widely used non-biological analyte sensing platforms. The realm of chemical sensing has been significantly augmented by the emergence of printable sensors based on metal oxides, presenting a sophisticated avenue for the detection and quantification of non-biological analytes. MOs sensors operate by detecting changes in the electrical conductivity of the material when exposed to specific target analytes. These sensors, rooted in the principles of materials science and nanotechnology, leverage the distinct properties of metal oxides to facilitate the transduction of chemical interactions into discernible signals, thereby enabling the sensitive and selective analysis of a diverse array of non-biological substances. These sensors have several advantages, including high sensitivity, fast response time, and low cost [6]. The status of MOs-based sensors is constantly evolving, driven by ongoing research and development efforts. Recent advances in materials science, nanotechnology, and device engineering have led to significant improvements in the performance and functionality of metal oxides [7]. MOs are a class of materials that have been widely used for printable chemical

sensors for non-biological analyte sensing. These sensors have several important properties that make them attractive for this application such as high surface area, chemical stability, selectivity, sensitivity, reversibility, low cost and printability [8]. These methods afford the deposition of finely tuned metal oxide nanoparticulate formulations onto diverse substrates, including flexible and cost-effective surfaces. The compositions and structures of oxides used in chemical sensors for non-biological analytes can vary depending on the specific sensing application and target analyte. The deployment of printable metal oxide-based chemical sensors for target analytes is found across an expansive spectrum of applications. Environmental monitoring, industrial process control, and gas-phase detection are domains where these sensors exhibit profound utility. The amalgamation of printable sensors with electronic readout systems facilitates seamless integration into data acquisition networks, thereby enabling real-time and remote monitoring capabilities.

1.1. Effects on the human body upon exposure to non-biological analytes

Exposure to various non-biological analytes can have different effects on the human body depending on the specific nature of the analyte, its concentration, duration of exposure, and individual susceptibility. Here are some general categories of non-biological analytes and their potential effects on the human body:

(a) *Toxic Gases (*e.g., *carbon monoxide, hydrogen sulfide)* [9]:

- Carbon Monoxide: Can lead to headaches, dizziness, nausea, confusion, and, at high levels, can result in unconsciousness or death due to its ability to bind to hemoglobin, reducing oxygen transport in the blood.
- Hydrogen Sulfide: Inhalation of high concentrations can cause respiratory irritation, headache, dizziness, nausea, and even unconsciousness or death. It is particularly hazardous due to its rapid onset of effects.

(b) *Volatile Organic Compounds (VOCs) (*e.g., *benzene, formaldehyde)* [10]:

- Benzene: Prolonged exposure to high levels can damage the bone marrow, potentially leading to anemia or leukemia.
- Formaldehyde: Can cause eye, nose, and throat irritation; long-term exposure may contribute to respiratory issues and certain types of cancer.

(c) *Particulate Matter (PM) and Dust* [11]:

- Inhalation of fine particulate matter can exacerbate respiratory conditions such as asthma and bronchitis. Long-term exposure is linked to cardiovascular diseases and lung function decline.

(d) *Heavy Metals (*e.g., *lead, mercury)* [12]:

- Lead: Can affect the nervous system, causing cognitive and developmental issues, especially in children.
- Mercury: Depending on the form (organic or inorganic), exposure can damage the brain, kidneys, and nervous system. It is particularly harmful to developing fetuses.

(e) *Industrial Chemicals (*e.g., *ammonia, chlorine)* [13]:

- Ammonia: Inhalation of high concentrations can cause irritation of the respiratory tract and eyes, leading to coughing, wheezing, and shortness of breath.
- Chlorine: Exposure to chlorine gas can lead to severe respiratory irritation, chest pain, and even pulmonary edema.

Immediate symptoms might include irritation, headaches, nausea, and dizziness, while long-term exposure can lead to chronic health issues and exacerbation of pre-existing conditions. To mitigate risks, proper ventilation, personal protective equipment, and adherence to safety guidelines are crucial when dealing with non-biological analytes in various environments.

1.2. Criteria for evaluating MOs non-biological analytes sensor

A collection of parameters is utilized to depict the sensor's performance as shown in figure 1. The most crucial parameters are detailed below, accompanied by their respective definitions.

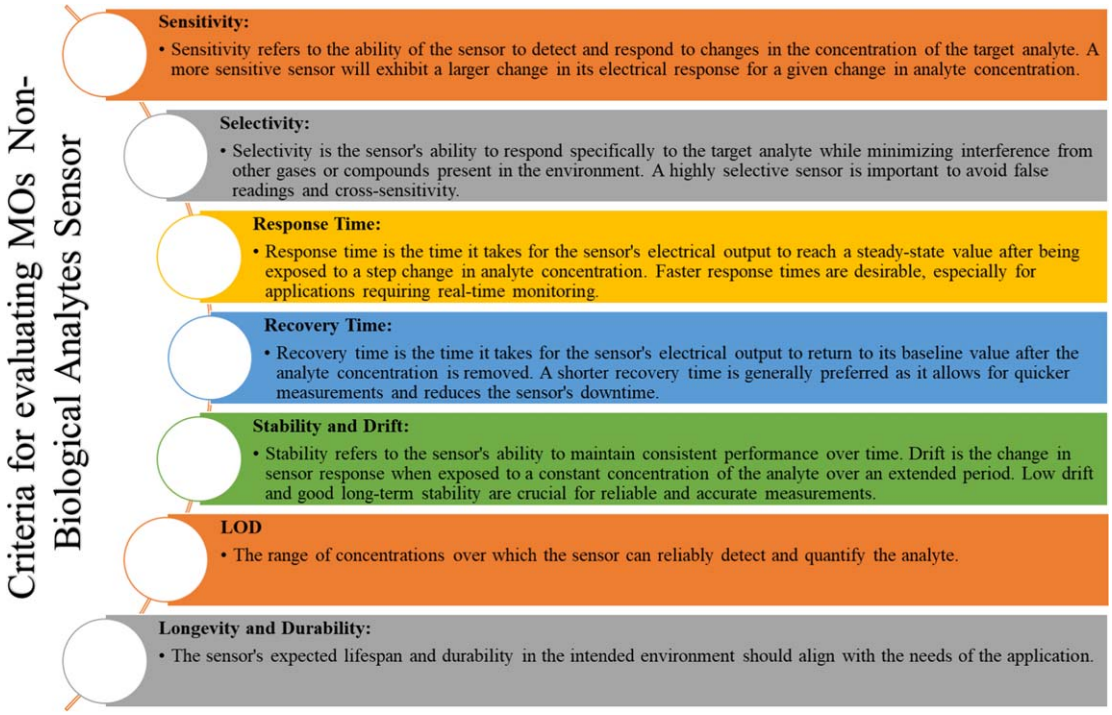

Figure 1. Criteria for evaluating MOs sensor performance.

1.3. General sensing mechanism for MOs non-biological analytes sensor

The fundamental basis of metal-oxide-based sensors is predominantly rooted in chemiresistance. This concept involves scrutinizing the alteration in electrical conductivity or resistivity of the material when exposed to an analyte (heavy metals ions, VOCs and toxic gases), contingent upon its concentration. The interaction between metal oxides and oxidizing or reducing gas molecules or ions brings about a decrease or increase in the resistance value of the metal oxide. Consequently, this mechanism effectively enables gas sensing capabilities. The detection mechanism in MOs gas sensors is associated with the ion sorption of substances onto their surfaces. When the gas sensor comes into contact with oxygen, the absorbed oxygen species are formed, causing the oxygen atoms to extract electrons from within the metal oxide. The subsequent steps (reactions 1–4) depict the kinetics of adsorption [14].

$$O_{2(abs)} \leftrightarrow O_{2(abs)}, \tag{1}$$

$$O_{2(abs)} \leftrightarrow O_2^-(ads)\ (\mathrm{T} \leqslant 150\ ^\circ\mathrm{C}), \tag{2}$$

$$O_2^-(ads) + e^- \leftrightarrow 2O^-(ads)\ (150\ ^\circ\mathrm{C} \leqslant \mathrm{T} \leqslant 300\ ^\circ\mathrm{C}), \tag{3}$$

$$2O^-(\mathrm{ads}) + e^- \leftrightarrow O^{2-}(\mathrm{ads})\ (\mathrm{T} \geqslant 300\ ^\circ\mathrm{C}) \tag{4}$$

When the MOs are exposed to the target analyte, the analyte interacts with the surface of the oxide, causing a change in the electrical properties of the material. This change in electrical properties is typically caused by the adsorption or chemisorption of the analyte on the surface of the MOs, leading to changes in carrier concentration, mobility, or conductivity. For example, some MOs sensors operate based on the chemical reaction between the analyte and surface, while others operate based on the physical adsorption or desorption of the analyte on the MOs surface. The sensing mechanism can also be influenced by factors such as temperature, humidity, and pressure, which can affect the adsorption and desorption kinetics of the analyte on the MOs surface. In light of these advancements, this review endeavors to comprehensively explore the intricacies of printable chemical sensors rooted in metal oxides for the detection of non-biological analytes. By delving into the nuanced mechanisms, fabrication methodologies, and application prospects, this review seeks to furnish a holistic understanding of the burgeoning landscape within this specialized domain, underpinning the critical role of printable metal oxide-based chemical sensors in modern analytical pursuits.

The conductivity of the sensing element is altered by the interaction between adsorbed oxygen and the reducing or oxidizing target analytes. In the presence of a reducing analyte, the adsorbed oxygen species on the sensing element detach and donate the previously trapped electron to the conduction band [15]. Consequently, the heightened concentration of electrons in the conduction band leads to a reduction in the resistance of the sensing element. Thus, when detecting reducing target analytes, n-type materials are favored, while p-type

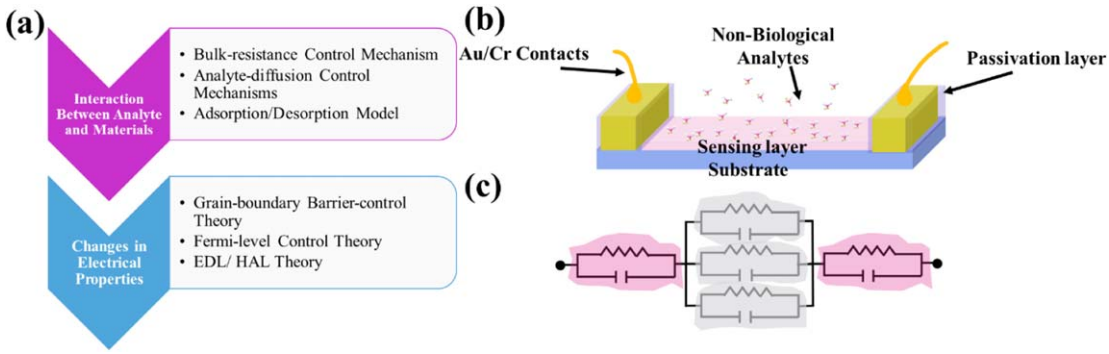

Figure 2. (a) Schematics of the sensing-mechanism categories (b) chemiresistive sensor with 4 main components: active material (sensing layer), contacts (Au/Cr), dielectric to insulate the contacts (passivation layer) and substrate (c) an electrical circuit of the chemiresistive sensor.

Table 1. Change in resistance of the semiconductor sensing element made from metal oxide when exposed to reducing and oxidizing analytes.

Metal oxide semiconductor	Reducing analytes	Oxidizing analytes
n-type	Resistance ↓	Resistance ↑
p-type	Resistance ↑	Resistance ↓

materials are chosen for the detection of oxidizing analytes. The selection of appropriate materials in conjunction with the target analyte requires careful consideration to enhance the sensor's performance characteristics. The changes in resistance of the sensing elements in response to reducing and oxidizing target analytes are summarized in table 1 [14]. In figure 2(a), the schematic representations of different categories of sensing mechanisms are depicted. In figure 2(b), the chemiresistive sensor is illustrated, comprising four primary components: an active material (sensing layer), contacts (Au/Cr), a dielectric layer for insulating the contacts (passivation layer), and a substrate. Figure 2(c) portrays the electrical circuit configuration of the chemiresistive sensor.

However, zinc oxide (ZnO) [16], tin oxide (SnO_2) [17], titanium dioxide (TiO_2) [18], tungsten oxide (WO_3) [19], and molybdenum oxide (MoO_3) [20] are commonly used for this purpose. The device architectures can be optimized by modifying the MO's material properties and device geometry, such as by changing the particle size, shape, and orientation, to improve the sensitivity, selectivity, and response time of the sensor. Hemoglobin trapped in hollow zirconium dioxide (ZrO_2) spheres and sodium alginate sheets electrodeposited on a gold electrode were used to create an H_2O_2 sensor [21]. This electrode produced a Hb $Fe^{3+/}Fe^{2+}$ quasi-reversible CV response. Methyl parathion, an organophosphate insecticide, was detected by using the high attraction between the zirconia and phosphate groups [22]. Maier have developed a flexible sensor for the detection of H_2O_2 in simulated breath, which has potential applications in health monitoring [23]. Liu Yang *et al* contrasted chemiresistive gas sensors with conventional methods for analyzing Chemical Warfare Agents (CWAs). These sensors offer notable advantages such as compact size, rapid response, and affordability in comparison to traditional instruments. Given the progress in nanofabrication technology and the emergence of novel sensing materials like carbon nanotubes, graphene, and black phosphorus (BP), the exploration of chemiresistive gas sensors remains a significant avenue of research [24]. Jae Eun Lee *et al* introduced a chemiresistive sensor based on a ZnO-CuO p-n heterojunction. This sensor configuration comprises CuO hollow nanocubes attached to ZnO spherical cores as the active materials. Notably, these core-hollow cube nanostructures made of ZnO-CuO display a remarkable response of 11.14 at 1 ppm acetone and 200 °C, surpassing the performance of other metal-oxide-based sensors reported in the literature. The response is measurable down to 40 ppb, and the limit of detection is estimated to be 9 ppb. Additionally, the ZnO-CuO core-hollow cube nanostructures exhibit strong selectivity toward acetone over other VOCs and maintain excellent stability for a period of up to 40 days [25].

Printable metal oxide nanostructures based chemiresistive non-biological analyte sensors can be designed using various device architectures, depending on the specific sensing application and target analyte. Here are some common device architectures used in such sensors as a thin film, nanoparticle, interdigitated electrode and flexible. This architecture involves printing or depositing sensing materials on flexible substrates, such as polymer films or fabrics, to create wearable or flexible sensors for non-invasive sensing applications. In

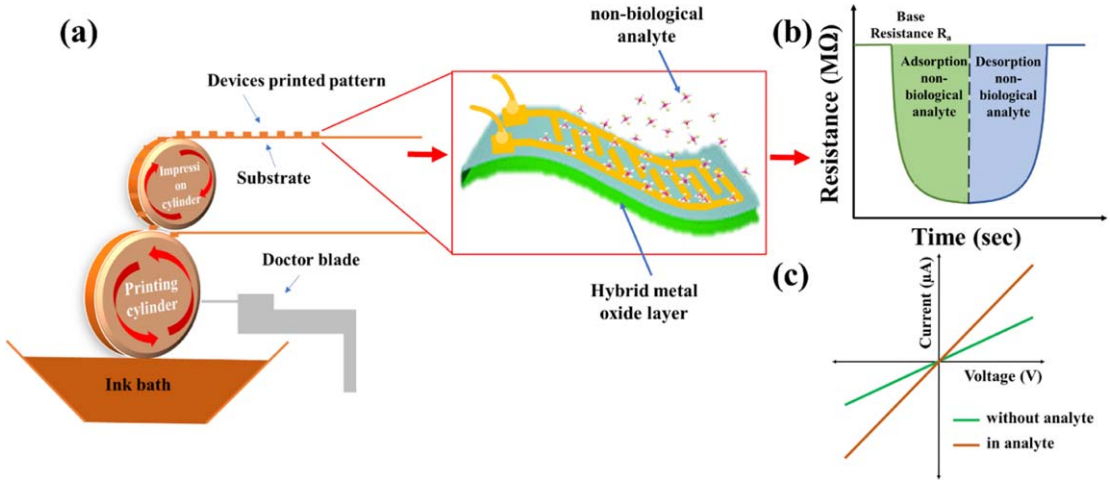

Figure 3. (a) Schematic diagram of printable chemical sensors for non-biological analytes on metal oxide. (b) change in resistance in the presence of target analyte (c) change in the current conduction in the presence of analytes and without analytes.

Table 2. Sensor performances for MOs nanostructures based chemiresistive non-biological analyte sensors.

Nanomaterial (MOs)	Analyte	Linear Range	Temperature	Detection Limit	References
Ca/Al-ZnO NPs	CO_2	0.25–5 RH%	200 °C	200 ppm	[26]
ZnO NRs	Phosphate	0.1 μM–7.0 mM	27 °C	0.5 mM	[27]
SnO_2/RGO nanocomposite	Cu^{2+}, Hg^{2+}	0.2 to 0.6 μM, 0.1 to 1.3 μM	—	2.269×10^{-10} M, 2.789×10^{-10} M	[28]
Au/Fe_3O_4-RTIL composite	arsenic	1−10 ppb	27 °C	0.0008 ppb	[29]
WO_3-SnO_2	chlorine	0.05–50 ppm	100 °C	0.05 ppm	[30]
MMM(ZIF-7/PEBA) coated TiO_2	formaldehyde	—	27 °C	0.0038 ppm	[31]
Cu_2O octahedral nanostructure	benzene	5-200 ppm	230 °C	5 ppm	[32]
CuO/SnO_2	H_2S	1–100 ppm	150 °C	1 ppm	[33]
rGO/WO_3-HFIP	DMMP	0.1–10 ppm	150 °C	0.1 ppm	[34]
Pd@ZnO	C_2H_5OH	100 to 1000 ppm	260 °C	100 ppm	[35]
2D/3D Bi_2MoO_6 micro-nano composites	trimethylamine	1.3–20 ppm	22 °C	1.3 ppm	[36]

figure 3(a), the schematic representation of printable chemical sensors designed for non-biological analytes on metal oxide is depicted. In figure 3(b), the alteration in resistance is presented when the target analyte is present, while figure 3(c) illustrates the modification in current conduction in the presence and absence of analytes.

The utilization of printable chemical sensors spans diverse applications, from environmental monitoring to industrial process control. By interfacing with non-biological analytes such as volatile organic compounds, heavy metals, and gas-phase molecules, these sensors contribute to enhanced detection sensitivity, reduced response times, and improved portability. Furthermore, the compatibility of printable sensors with electronic readout systems ensures seamless integration into data acquisition networks, enabling real-time monitoring and analysis. Zhennan Zhu *et al* have devised functional ink systems based on metal oxides tailored for precision drop-on-demand printing of thin-film transistors. Their work encompasses an extensive review of distinct ink systems utilized in the context of thin-film transistor printing. Simultaneously, the study provides a comprehensive analysis of challenges encountered in the domain of printed thin-film transistors, accompanied by elucidation of resolutions originating from the ink system perspective [9]. Table 2 displays some reports on the sensor performances for non-biological analytes based on MOs nanostructures.

2. Current and future challenges

Despite the potential advantages of printable MOs nanostructures based chemiresistive non-biological analyte sensors, several current challenges need to be addressed to improve their performance and practicality [37]. Figure 4 shows the development of effective sensing characteristics along with the accompanying challenges.

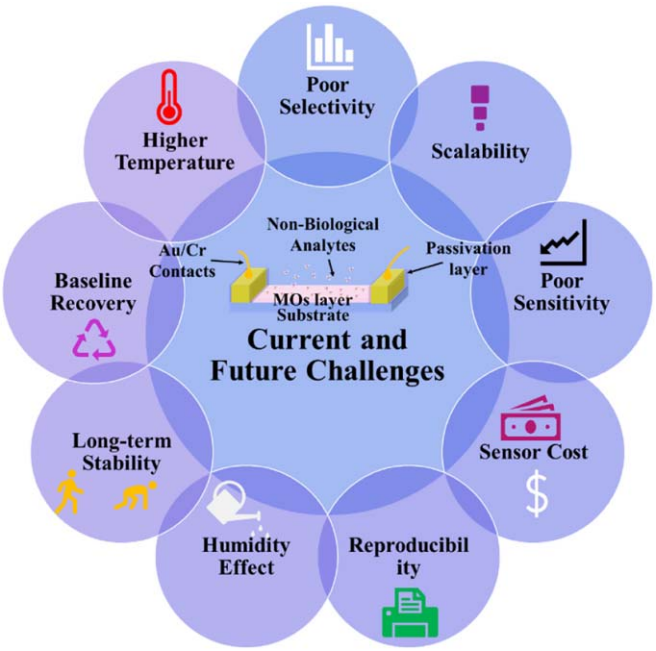

Figure 4. Development of effective sensing characteristics along with the accompanying challenges.

Some of these challenges include selectivity, sensitivity, long-term stability, reproducibility, baseline recovery, humidity effect, high temperature, cost and scalability [38]. One of the main challenges in the development of sensors is achieving high selectivity towards the target analyte while avoiding interference from other chemical species present in the sample matrix. Metal-oxide sensors have a sensitivity range of parts-per-million (ppm) or even parts-per-billion (ppb), which allows them to detect non-biological analytes at low concentrations. The operating temperature, which must be precisely managed to provide optimal performance, has a significant impact on their sensitivity. In general, higher working temperatures increase sensitivity, but they can also result in decreased selectivity and shortened sensor lifetime. Additionally, metal oxide sensors can exhibit cross-sensitivity to other analytes, which can lead to false-positive or false-negative results. With metal-oxide sensors, reproducibility is also a serious problem since changes in fabrication parameters or ambient factors can significantly alter sensor performance. To solve this, rigorous quality assurance processes should be used during the sensor production process. Additionally, calibration techniques should be used to take into account changes in sensor performance over time. This requires optimizing the MOs morphology, porosity, and size, as well as the operating conditions such as temperature and humidity. Additionally, there are challenges in scaling up the production of these sensors to meet industrial demand. Therefore, it is essential to explore cost-effective and scalable fabrication methods, such as inkjet printing or roll-to-roll processing.

SnO_2 is a metal oxide that is frequently used in non-biological sensors, although it is susceptible to interference from humidity and other analytes, which can lower its selectivity towards particular target analytes. On the other hand, it has been demonstrated that zinc ZnO [47] sensors have a higher sensitivity to some analytes, although they can be less repeatable due to fluctuations in the growth conditions of the thin films used in their production [48]. While the selectivity and sensitivity of other metal oxides, such as tungsten oxide (WO_3) [49] and titanium dioxide (TiO_2) [50], have shown encouraging results, other variables, including the crystal structure, doping concentration, morphology and operation temperature, can also affect how well these materials work. There is a growing demand for sensors that can be used in portable or handheld devices for on-site and in-field applications. Therefore, future challenges in this area will involve developing sensors that are small, lightweight, and low power-consuming, while maintaining high sensitivity and selectivity. Based on recent research, the synthesized cabbage-like ZnO nanostructure electrode shows potential as an auspicious candidate for use in innovative chemical sensors designed to detect harmful chemicals, such as resorcinol. These findings suggest that the ZnO nanostructures electrode could serve as an efficient and effective tool for detecting resorcinol in various applications, highlighting its potential as a valuable addition to the field of chemical sensing. Although the sensor's detection range (5 μM–320 μM) exceeds the H_2O_2 concentration in human breath (0.1 μM–1.5 μM in the case of exhaled breath condensate), it serves as proof of concept for a commercial sensor [51]. Overall, addressing these current and future challenges will require continued research and development in materials science, chemistry, physics, and engineering, as well as collaboration across different

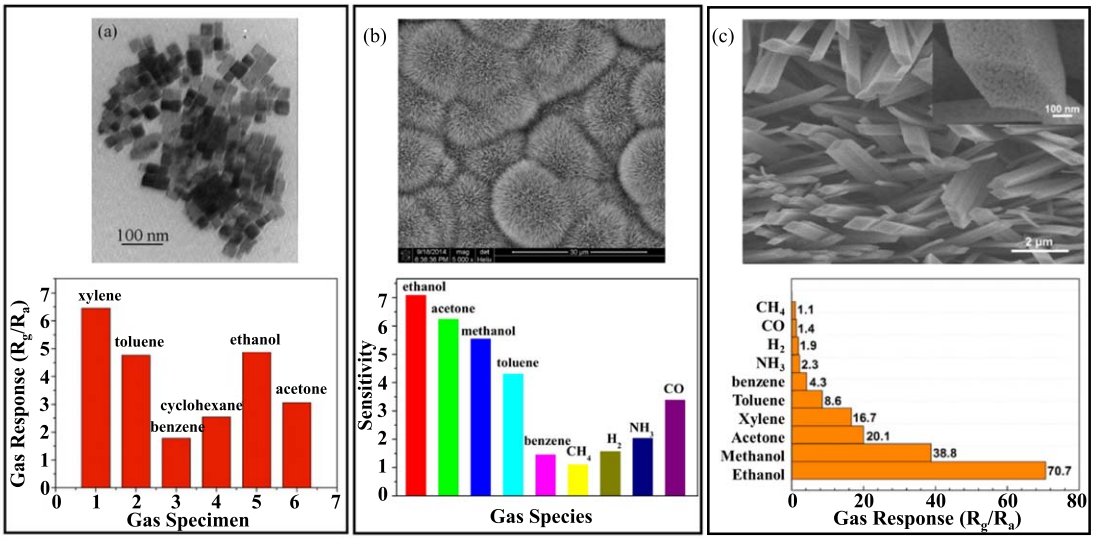

Figure 5. (a) Cubic shaped morphology of Co_3O_4 [39] Copyright 2011, Elsevier (b) urchin-like morphology of Co_3O_4 [40] Copyright 2017, Elsevier (c) rhombus-shaped morphology Co_3O_4 NR and their selectivity respectively [41] Copyright 2013, Elsevier.

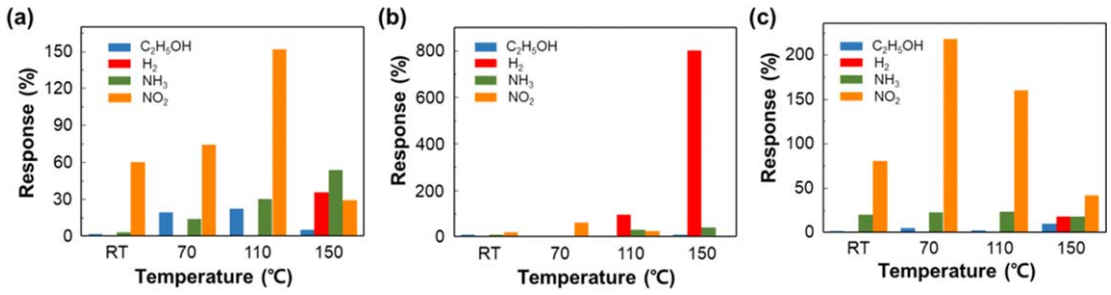

Figure 6. (a) Gas sensing responses for a $PMoS_2$, (b) Pd/MoS_2, and (c) Au/MoS_2 toward 500 ppm C_2H_5OH, 500 ppm H_2, 500 ppm NH_3, and 50 ppm NO_2 as a function of operating temperature [42] Copyright 2019, Springer.

fields and industries. By overcoming these challenges, printable metal oxide nanostructures-based chemiresistive non-biological analyte sensors have the potential to revolutionize sensing and monitoring in a wide range of applications, from healthcare to environmental monitoring to industrial process control. Detecting non-biological analytes presents numerous challenges due to their low concentrations, differential appearance in cells, multi-step sanitization procedures, and the use of expensive reagents. Consequently, there is a growing interest in the research and development of novel sensing materials that surpass the capabilities of traditional sensing materials, alongside investigations into the underlying sensing mechanisms. Metal-oxides non-biological analytes sensors are often characterized by limited selectivity towards different analytes, whereas emerging two-dimensional (2D) transition metal dichalcogenides materials encounter challenges such as reduced sensitivity, difficulties in large-scale production, and poor stability [52].

2.1. Morphology dependent selectivity

One of the main challenges in the development of sensors is achieving high selectivity towards the target analyte while avoiding interference from other chemical species present in the sample matrix. Selectivity stands as one of the utmost critical performance metrics in the realm of trace target analyte sensing. Selectivity, or the ability of a gas sensor to specifically respond to a target gas while ignoring interference from other gases, is a critical aspect of gas sensing technology.

Diverse synthesis and fabrication methods have been employed to create gas sensor materials with distinctive morphologies, potentially impacting their selectivity. A compilation of these investigations aims to assess how synthesis and morphology exert an influence on sensor selectivity. While the subsequent section will primarily concentrate on p-type metal oxides due to their frequent application for enhanced chemical sensitization, it's important to note that the discussion of pristine n-type materials will also consider how morphology can impact their response. This focus on p-type oxides arises from their comparatively limited

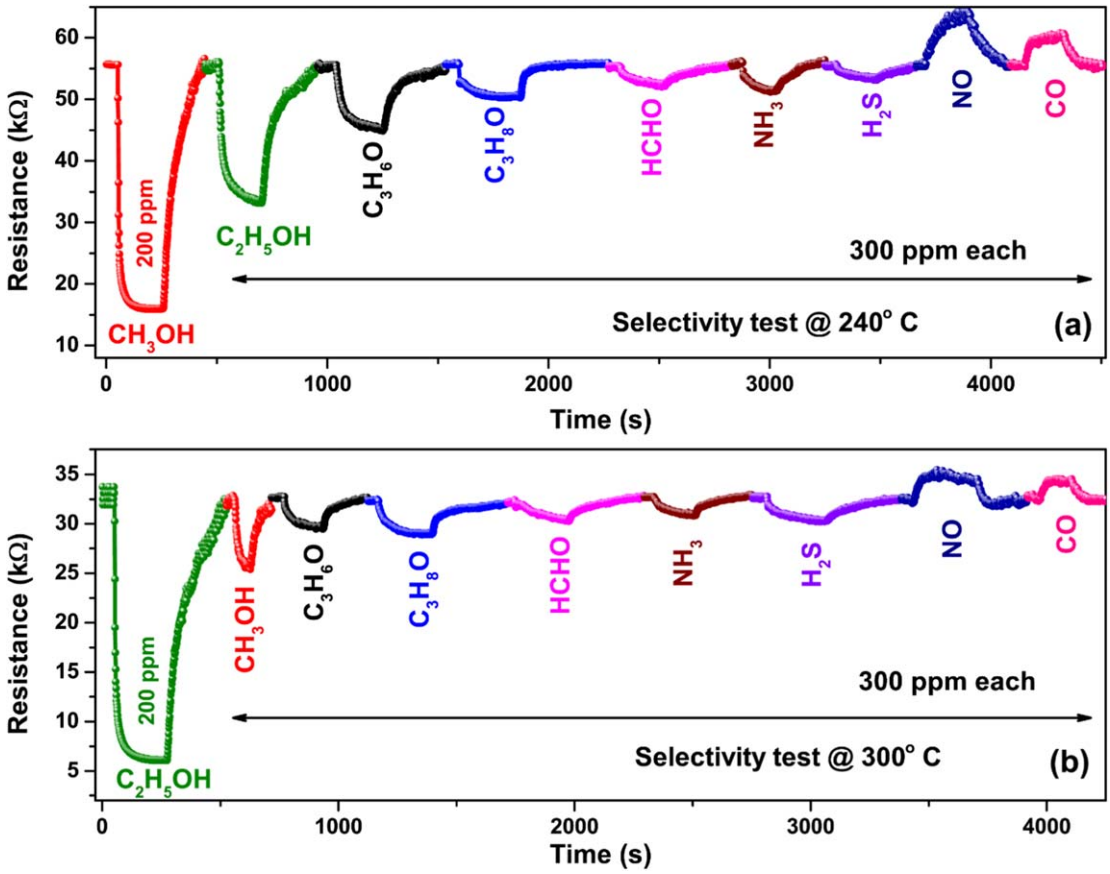

Figure 7. Selectivity of the MoS_2/TiO_2 nanocomposite-based sensor towards 200 ppm of methanol and ethanol (a) Temperature = 240 °C and (b) Temperature = 300 °C [43] Copyright 2013, Elsevier.

exploration in the existing literature. In figures 5(a)–(c) we can see that how morphology changes as its gas changes. While the characterization of exposed facets was lacking in numerous investigations, it is evident that the growth mechanisms frequently mentioned might provide insights into how the crystallographic facets of Co_3O_4 contribute to the alteration of selectivity between ethanol and acetone.

2.2. Temperature dependent sensitivity

This requires careful optimization of the material's composition, structure, and surface properties, as well as the design of appropriate sensing. The sensitivity of metal oxide-based sensors is intricately linked to the sensing temperature due to the dynamic changes that occur in the material's surface and electronic properties within varying temperature ranges. Sensing temperature significantly influences the kinetics of chemical reactions occurring at the surface of metal oxide sensors, subsequently affecting their interaction with target analytes. At elevated temperatures, the chemical reactions between the metal oxide surface and the target analyte molecules tend to be more favorable and efficient. This often leads to enhanced adsorption, desorption, and catalytic processes, resulting in increased sensitivity and response towards the analytes. Higher temperatures can also facilitate the release of adsorbed molecules from the surface, making the sensor more responsive to subsequent analyte exposures.

Jun Min Suh *et al* delved into the impact of Pd and Au decoration on the gas-sensing characteristics of MoS_2 thin films [42]. The introduction of Pd and Au decoration proved effective in reducing the operational temperature required to attain the utmost gas response to NO_2. This was achieved by electronically sensitizing the MoS_2 material. Additionally, the incorporation of Pd decoration led to a substantial enhancement in selectivity towards H_2, accomplished by the formation of Pd hydride as shown in the figure 6(b). Furthermore, Au decoration yielded an improvement in the overall gas responses across all tested gas species as shown in the figure 6(c). Notably, alterations in conduction types (n-type or p-type) were observed contingent on the specific gas species and operational temperatures. This study elucidates the discernible impacts of noble metal catalyst decoration on the gas sensing properties of MoS_2, offering valuable insights into the field [42]. In the recent advancement in the material science the sensor shows dual sensing behaviour.

Sukhwinder Singh *et al* investigated the gas-sensing performance of the MoS_2/TiO_2 hybrid that was prepared, measuring it across varying temperatures as shown in the figures 7(a), (b) [43]. Interestingly, the device exhibited distinct detection of methanol and ethanol at different temperatures, showcasing a selective response. This selectivity phenomenon is possibly attributed to the alignment between the LUMO (least unoccupied molecular orbital) energy of the adsorbed analyte and the adsorbed oxygen on the sensor's surface. This preference could arise from the matching electronic energy levels between the LUMO energy of these two analytes and the adsorbed oxygen on the device's surface. The LUMO energies for methanol and ethanol are 0.197 and 0.125 eV, respectively. Hence, the interaction of adsorbed gaseous species with the sensor surface, involving electron transfer, is significantly influenced by the LUMO energies of the respective gas molecules. This interaction depends on factors like the operational temperature, as well as the inherent electronic characteristics of the sensing channel. For instance, elemental semiconductors exhibit a decrease in band gap with increasing temperature, which augments their conductivity. In this context, a higher operating temperature can enhance the charge transfer between adsorbed gaseous species and the sensing surface, potentially leading to selectivity due to the varying LUMO energies of different gas molecules. Consequently, by capitalizing on temperature-induced high selectivity and a substantial response value of MoS_2/TiO_2 against a spectrum of seven distinct gas analytes, practical applications in the medical domain could be unlocked [43].

2.3. Reproducibility

Reproducibility of a sensor refers to its ability to consistently provide similar measurements or responses when exposed to the same conditions or analytes across multiple trials. A highly reproducible sensor yields results that exhibit minimal variation between repeated measurements, indicating its reliability and accuracy. Kyungjae Lee *et al* worked on the precision of reproducibility that was validated by employing multiple devices (depicted in figure 8(a)) and conducting multiple experimental runs (illustrated in figure 8(b)) [44]. Notably, the data obtained from these repeated runs also shed light on the regeneration capabilities of the receptor surface. The regenerative process required careful treatment, where purging with N_2 was exclusively used to eliminate layers of DNT (dinitrotoluene) gas molecules while preserving the immobilized peptide (aptamer) intact. For the experimentation involving multiple devices (figure 8(a)), a DNT-bp (DNT-binding peptide) rGO sensor was prepared. The process entailed an initial stabilization of resistance change (5 min), followed by the introduction of 320 ppb DNT vapor (5 min), succeeded by a N_2 gas purge (10 min), iterated five times across multiple rGO sensor chips ($N = 5$). The calculated average resistance change for these five rGO sensors was approximately 98.8×10^{-4}, accompanied by a standard deviation of about 0.13%. Furthermore, the coefficient of variation (C. V.) was determined as 13.8% from the data obtained across multiple rGO sensor chips, indicating a commendable level of reproducibility. Similarly, in the case of multiple experimental runs (figure 8(b)), reproducibility was assessed using the same rGO sensor and following the protocol outlined in figure 6(a). The calculated average resistance change resulting from the interaction between DNT-bp and DNT gas was approximately 99.6×10^{-4}, exhibiting a standard deviation of around 2.3×10^{-4}. The C.V. was computed at approximately 2.30% from multiple rGO sensor chips, indicating a high level of reproducibility [44].

2.4. Humidity effect

At higher humidity conditions, the baseline of a MOs sensor often does not remain stable due to the influence of water vapor on the sensor's surface and electrical properties as we can see in the figure 9 where the sensor baseline not reaching to its initial value. The gradual elevation of the base resistance (Ra) in both pure and Pt-anchored $CuCrO_2$ chemiresistors is a consequence of the retrieval of primary hole carriers (generated thermally). This phenomenon arises through the subsequent reaction [46]:

$$OH^- + h^+ \rightarrow \cdot OH \tag{5}$$

Given that ·OH radicals exhibit potent oxidizing characteristics, the reaction kinetics of chemiresistors towards reducing H_2S experience significant augmentation in the presence of a humid air atmosphere, as evidenced by figure 9. This phenomenon can be attributed to several factors such as the adsorption of water molecules, surface ionization, chemical reactions. However, it's important to recognize that in high-humidity environments, the behavior of MOs sensors can become complex due to the interaction between water vapor and the sensor surface, leading to deviations from a steady baseline.

To overcome these limitations, a promising research direction could be the integration of traditional materials such as 2D Black Phosphorus [53], Ti_3C_2 MXene-Polymer [54], 2D MOF nanosheets, and carbon-based materials with 2D materials to enable more effective non-biological analytes detection.

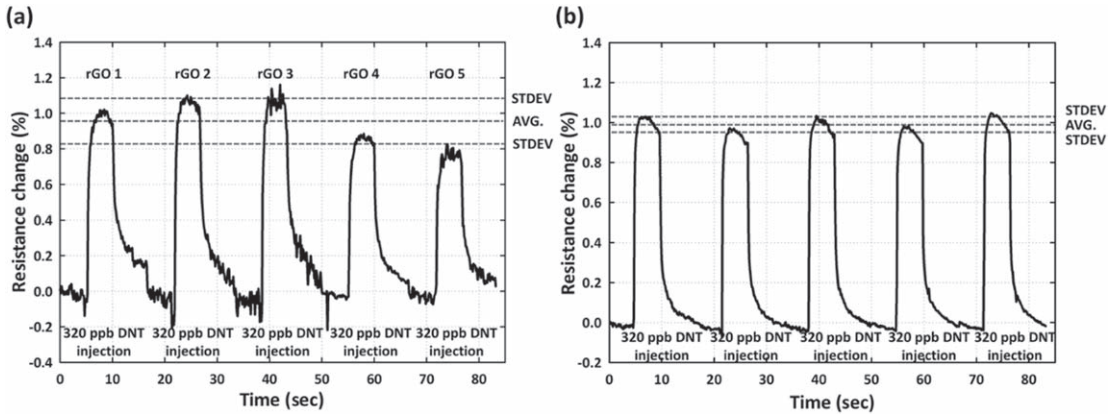

Figure 8. DNT-bp sensor reproducibility and regeneration test for (a) multiple devices and (b) multiple runs. The resistance change measured during multiple runs is reproducible (shown here for 320 ppb DNT), and the trace in (b) also confirms the complete regeneration of the sensor surface between successive runs at room temperature by using N_2 gas [44] Copyright 2019, Nature.

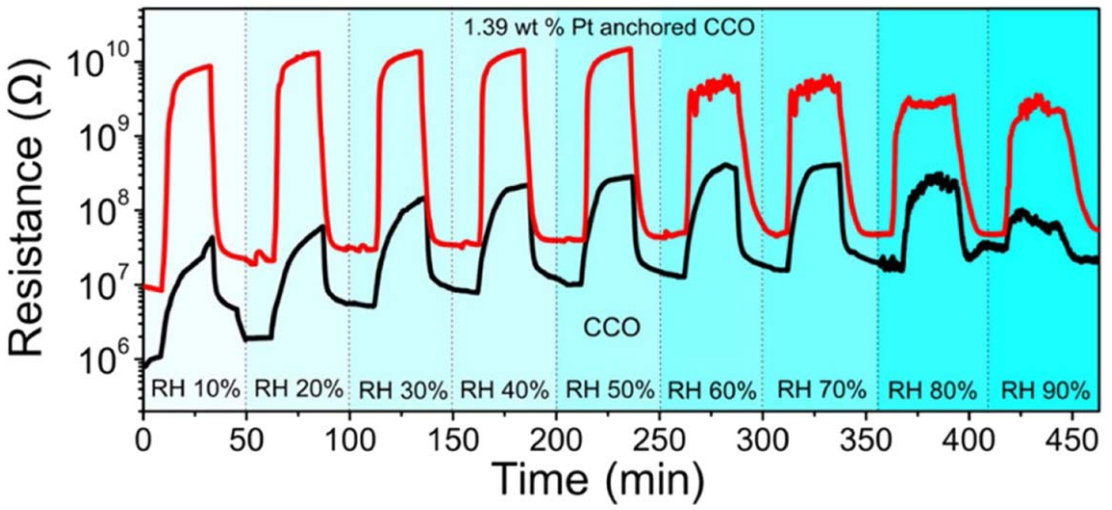

Figure 9. Response curves of pure and 1.39 wt % Pt-anchored $CuCrO_2$ chemiresistors to 10 ppm H_2S under different relative humidity levels [45] Copyright 2022, ACS.

3. Advances in science and technology to meet challenges

The developed non-biological analytes chemical sensors are currently in the prototype stage and have solely been evaluated in laboratory settings. The number of actual samples used for evaluation has been minimal, rendering validation inadequate. The development of marketable products is contingent upon addressing challenges about optimizing the stability, storage, and logistics of the printable chemical sensors for non-biological analytes, as well as ensuring their optimal performance in minimally treated or diluted diverse samples. Recent developments in materials science have led to the development of a new class of materials, termed 'nanocomposite materials', which are composed of organic semiconductors and biomass derivatives. These hybrid materials exhibit superior unique properties such as high electrical conductivity, robust mechanical strength, and excellent thermal stability [55]. Chemical sensing devices face significant challenges regarding selectivity and sensitivity. Therefore, there is a pressing need to integrate interdisciplinary fields to create smarter and high-performance chemical sensing devices. The emergence of nanotechnology, which involves the manipulation and control of materials at the atomic and molecular level (typically in the nanometer range), has led to exciting developments in non-biological analytes design. The synthesis of materials at the nanoscale has enabled the exploitation of exceptional physical, chemical, and biological properties, which are central to the success of nanotechnology.

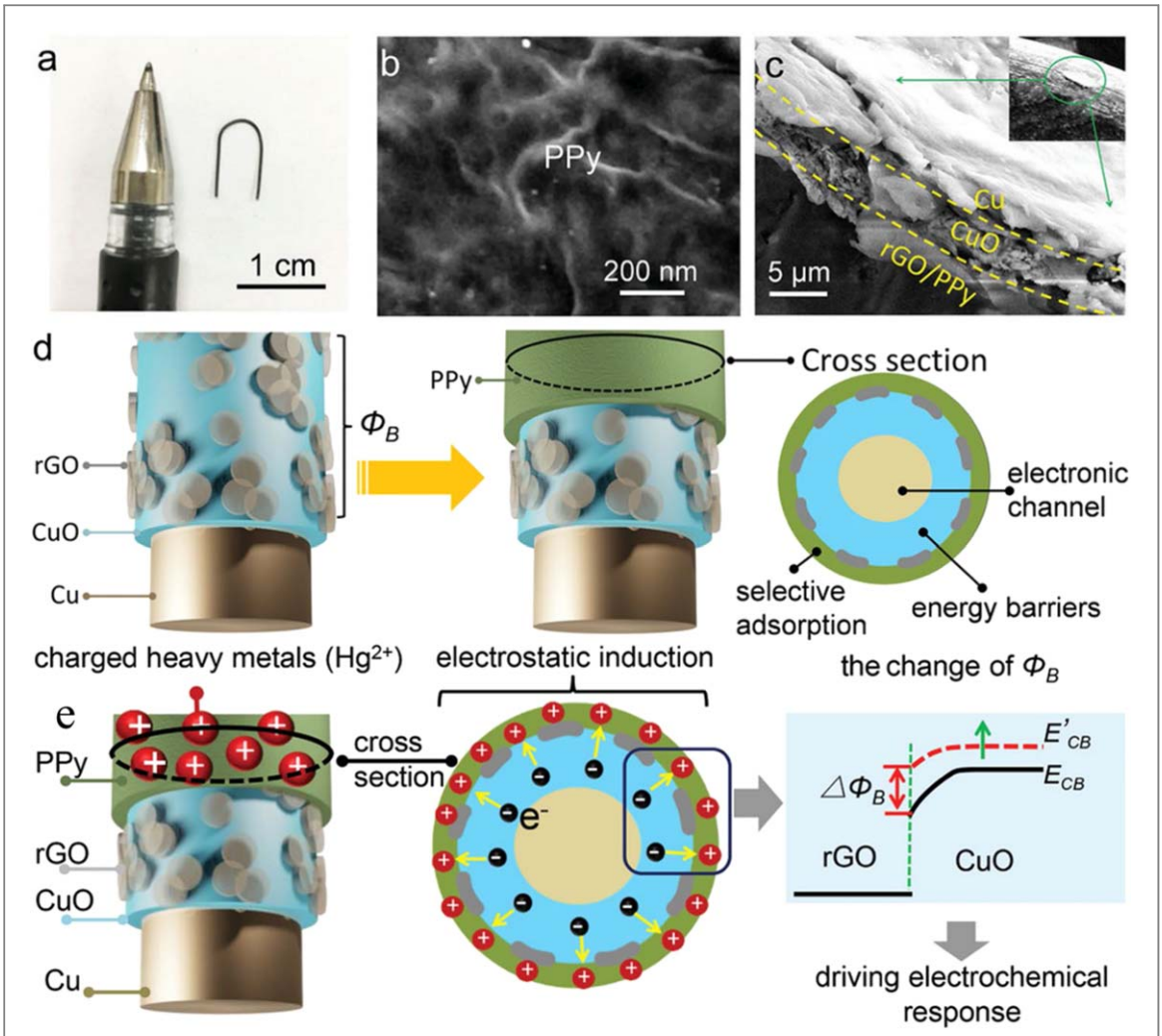

Figure 10. (a) The macroscale photo of the Cu/CuO/rGO/PPy wire. (b) The SEM image of the surface of a Cu/CuO/rGO/PPy wire. (c) The locally magnified SEM image of the peeled surface of the Cu/CuO/rGO wire. (d) The schematic diagram of the Cu/CuO/rGO/PPy wire. The Cu wire (brown cylinder) in the core acts as the electron transport channel; the CuO (blue shell) and the rGO (semitransparent grey tablets) act as the heterojunction; the PPy (the outmost green shell) as the selective adsorption layer. (e) The schematic diagram of the physical-electrochemical sensing mode for detection of heavy metals (Hg^{2+}). After the specific adsorption of Hg^{2+} on the PPy layer, the formed positively charged layer traps electrons from the exposed CuO by electrostatic interaction, which raises the conduction band of CuO, and increases the Φ_B [62] Copyright 2020, Wiley.

3.1. Advances in material science

For the non-biological analytes sensing characteristics of the different MOs can be presented, focusing on strategies such as metal doping (Au, Ag, Pd, Pt) [56, 57], nanohybrid structure [58], nanocomposite [58], heterojunction composites (n-n, p-p, n-p) [59, 60], defects in nanomaterials, and different morphologies [61] that are applied to enhance their sensing characteristics.

Minggang Zhao *et al* have constructed distinct hierarchical structures, namely Cu/CuO/rGO/PPy, Cu/CuO/rGO/CS, and Ni/NiO/ZnO/PPy, successfully incorporating various interfacial energy barriers, such as Schottky or p-n junctions, within electrochemical sensors as shown in the figures 10(d), (e) [62]. These structures enable the modification of energy barrier heights through electrostatic interactions between charged analytes and the interfacial junctions. This adjustment corresponds to the specific charged analytes, ultimately amplifying the electrochemical response of the sensors in an exponential manner. Unlike conventional redox-based electrochemical sensors, the novel sensing mechanism grounded in interfacial energy barriers possesses a distinctive feature—resistance to interference in intricate scenarios, including environments like seawater. Engineered absorbing layers, such as PPy (polypyrrole) for Hg^{2+} and CS for Cu^{2+}, are specifically designed to accumulate analytes and their charges. These charges' electrostatic induction can impact the interfacial energy barrier without necessitating redox reactions. This newly established sensing mode boasts exceptional anti-interference properties and ultra-high sensitivity as shown in figures 11(c), and (d), thus presenting novel avenues for detecting trace analytes within challenging settings like seawater [62].

In their study, Ana Zubiarrain *et al* have shown that graphene-like carbon (GLC) can serve as the basis for constructing chemiresistive sensors capable of detecting free chlorine in water across a wide concentration range

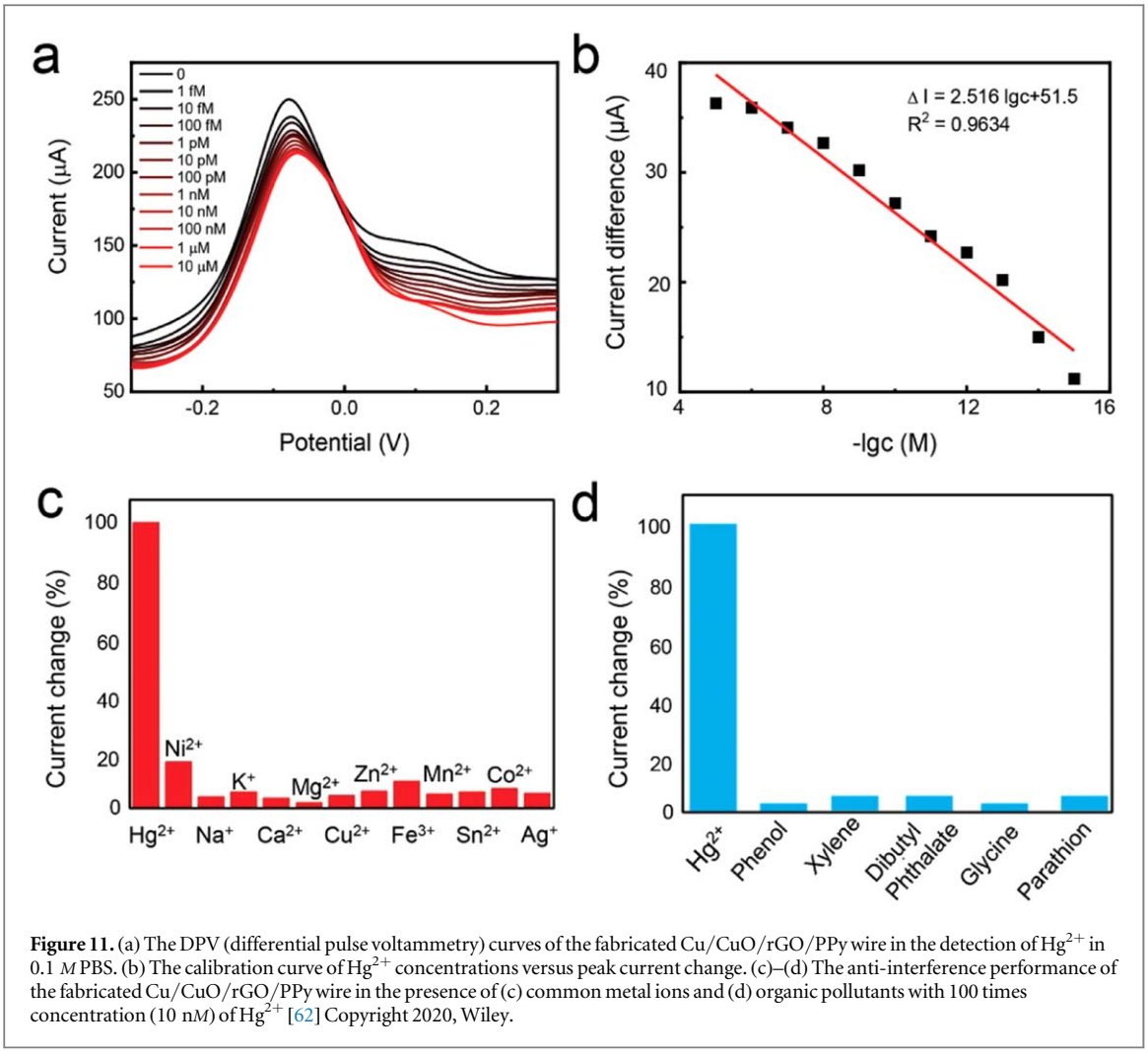

Figure 11. (a) The DPV (differential pulse voltammetry) curves of the fabricated Cu/CuO/rGO/PPy wire in the detection of Hg^{2+} in 0.1 *M* PBS. (b) The calibration curve of Hg^{2+} concentrations versus peak current change. (c)–(d) The anti-interference performance of the fabricated Cu/CuO/rGO/PPy wire in the presence of (c) common metal ions and (d) organic pollutants with 100 times concentration (10 n*M*) of Hg^{2+} [62] Copyright 2020, Wiley.

as shown in the figures 12(a)–(d) [63]. They examined the sensor responses within two distinct concentration ranges: 0.01–0.2 ppm and 0.2–1.4 ppm as shown in the figure 12(e). The thickness of the GLC films had a notable impact on the maximum sensor response and saturation concentrations, with thinner films proving more sensitive but offering a narrower detection range. The thinnest GLC films (12 nm) achieved an impressive limit of detection, as low as 1 ppb. Detecting concentrations exceeding 1.4 ppm seemed feasible with GLC films thicker than 46 nm. These sensors didn't require external resetting and exhibited a reduction in response when exposed to lower free chlorine concentrations, making them suitable for monitoring concentration variations. Although bare devices showed some response to free chlorine, functionalizing them with phenyl-capped aniline tetramer (PCAT) substantially enhanced their performance in quantifying free chlorine in actual tap water samples. In a specific case, the blank devices estimated a water sample containing 0.4 ppm chlorine to be 0.6 ± 0.1 ppm, while the doped sensors estimated it as 0.4 ± 0.1 ppm as shown in figures 12(g), (h).

Furthermore, the sensors exhibited negligible responses to common cations and anions found in drinking water, with signal changes being less than 5% in response to 0.5 ppm of free chlorine. The versatility of GLC-based chemiresistive sensors is exemplified by their ability to adapt sensitivity and dynamic range through varying GLC film thickness. This flexibility opens up various applications, including real-time water quality monitoring, chlorine filter breach detection, and quantifying free chlorine in unknown samples. Their ultra-low power consumption (less than 100 nW during reading) makes them ideal for remote monitoring applications. Moreover, the design of these chemiresistive sensors isn't confined to free chlorine alone; the nanocarbon films can be tailored for other specific chemical targets. Additionally, the study demonstrated the use of two different sensor geometries, expanding deployment possibilities. While the manual, lab-based fabrication method used in this study exhibited some variation in response magnitude between devices due to narrow tolerances, the film format of GLC holds the potential for cost-effective mass production of sensors in the future [63].

Pil Gyu Choi *et al* achieved the synthesis of Co_3O_4 nanoparticles through a hydrothermal process, with the growth of these nanoparticles being controlled by crystal formation [64]. Figure 13(a), shows the schematic depiction of an irregularly shaped structure, alongside the alteration in resistance when an analyte is present.

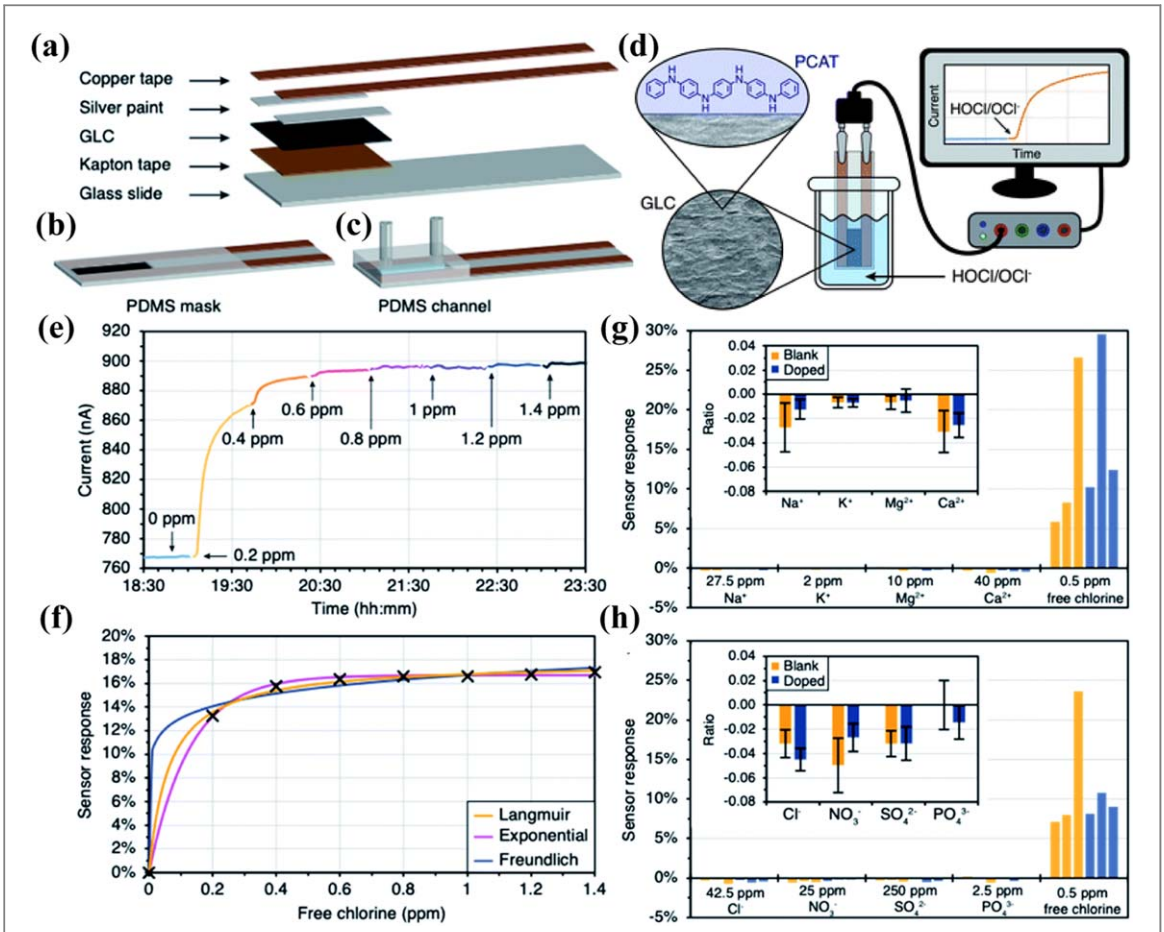

Figure 12. (a) Fundamental elements of chemiresistive sensor (b) Dip sensor structural design (c) Flow sensor structural. (e) unprocessed data acquired from a doped sensor with a 12 nm thickness of graphene-like carbon (GLC) and a 100-mV bias (d) Setup for automated surveillance of free chlorine levels in drinking water (f) Fitting calibration curves to Langmuir adsorption isotherms, exponential decay models, and Freundlich adsorption isotherms (g) reaction of a doped sensor to an actual drinking water sample and the concentrations artificially introduced afterwards (h) Mean concentrations foreseen by the sensor with and without contamination, with the actual sample concentration depicted by the purple line, and the standard deviations of sensor readings shown as error bars (all measurements conducted using 24 nm GLC at 10 mV) [63] Copyright 2022, RSC.

Moving on to figure 13(b), presents a schematic representation of a structure under crystal growth control, which displays enhanced sensing capabilities following the introduction of crystal defects, accompanied by a change in resistance when exposed to an analyte. During this process, three distinct raspberry-type structures, a cubic shape, and an irregular form emerged within the Co_3O_4 nanoparticles. It was observed that the raspberry-type Co_3O_4 structures exhibited a smaller crystallite size compared to the cubic and irregular variants. This divergence in size could be attributed to the raspberry-type structures possessing a larger lattice volume, a phenomenon resulting from lattice expansion due to the presence of crystal defects. Notably, the presence of these crystal defects yielded an enhancement in gas sensing attributes, particularly towards reducing gases like H_2, C_5H_8, and CH_3COCH_3, in contrast to the acidifying gas NO_2 as shown in figure 14(f). Additionally, the hierarchy of gas sensor signal responses shifted as crystal defect areas increased on the Co_3O_4 surface. The affinity of a gas molecule's higher dipole moment exerted a more potent influence of crystal defects on gas sensing properties. Furthermore, these crystal defects displayed sensitivity to humidity, where water molecules at crystal defect sites and adsorbed H_2O interacted with target gas molecules, enhancing polar molecule adsorption as shown in figures 14(a)–(e). The Co_3O_4 nanoparticles, controlled through crystal growth, exhibited comparable durability to the irregularly shaped variants. These findings hold the potential to contribute significantly to comprehending the gas-sensing properties of Co_3O_4, particularly those tied to surface states. Furthermore, these insights hold promise for applications spanning human healthcare and environmental protection. These applications include selective sensing of specific target gas molecules such as NO_2 for environmental acidification, CH_3COCH_3 for diabetic ketoacidosis diagnosis, C_5H_8 for elevated blood cholesterol, and H_2 for colonic flora [64].

Ruofan Zhang *et al* have developed a solution combustion synthesis (SCS) approach to create porous Pt-anchored $CuCrO_2$ (CCO) nanoparticles in a single step [45]. This process enables atomic-level mixing of reactants and Pt ions, facilitating the even dispersion of Pt atoms within the CCO matrix. Employing an

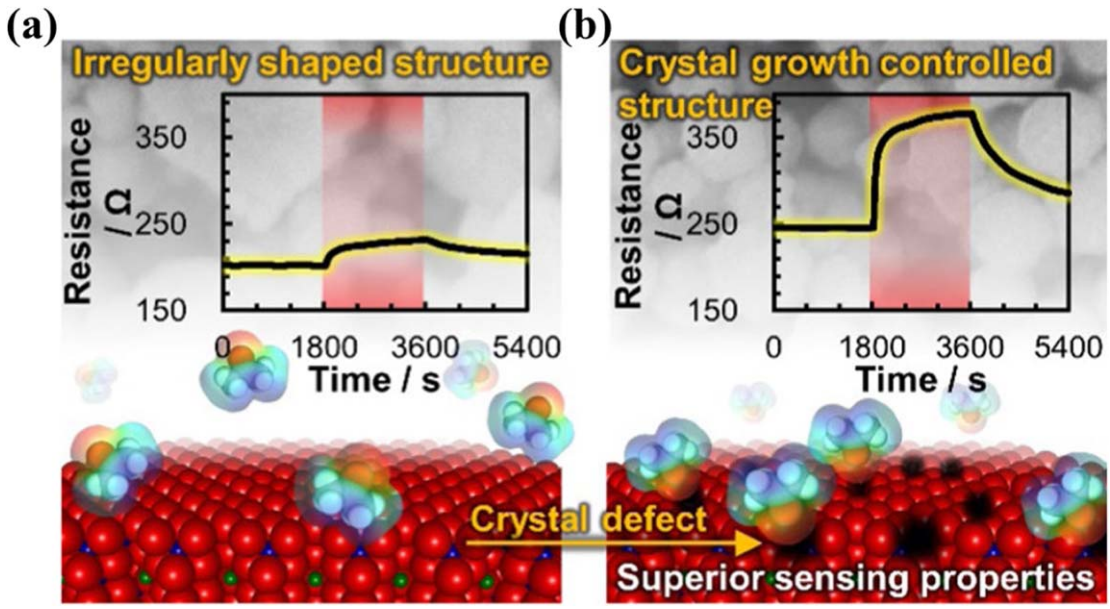

Figure 13. (a) Schematic representation of irregularly shaped structure and change in resistance in the presence of analyte (b) schematic representation of crystal growth-controlled structure after the crystal defect and change in resistance in the presence of analyte show the superior sensing [64] Copyright 2020, ACS.

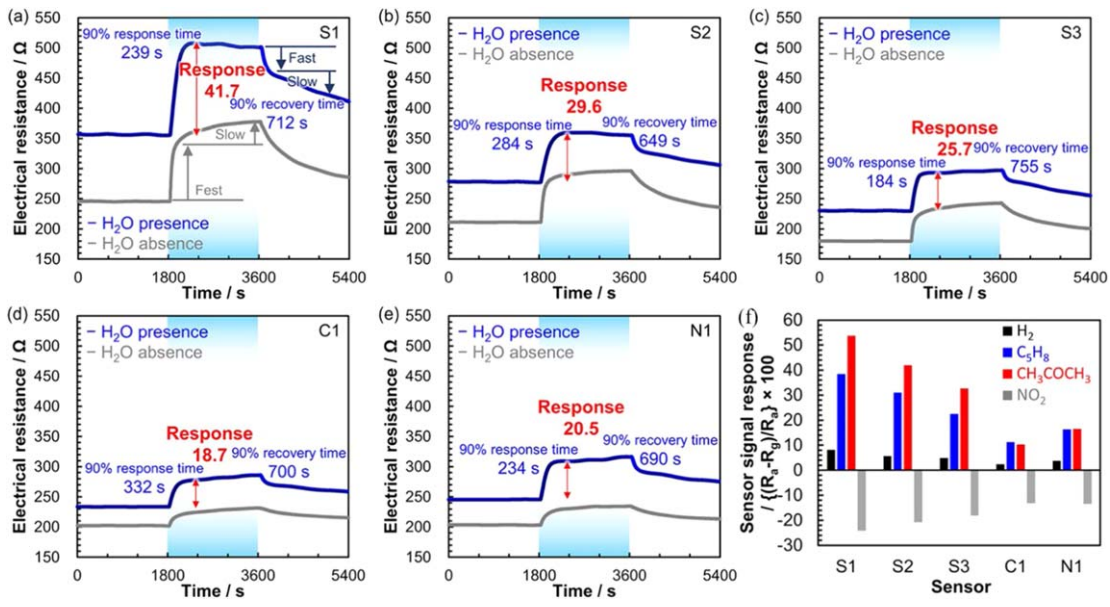

Figure 14. Resistance variations of (a) S1, (b) S2, (c) S3, (d) C1, and (e) N1 for 20 ppm CH_3COCH_3 gas in the presence of H_2O. (f) Sensor signal response to 20 ppm H_2, C_5H_8, CH_3COCH_3, and NO_2 gases [64] Copyright 2020, ACS.

optimized Pt ratio of 1.39 wt %, Pt-anchored CCO nanoparticles significantly enhanced response characteristics towards H_2S. This enhancement includes a remarkable 1250-fold increase in response from 10 ppm H_2S at a low operating temperature of 100 °C 35 times higher than pure CCO as we can see in figure 15(a). Additionally, the Pt-anchored CCO exhibited excellent selectivity and reproducibility shown in figure 15(b) [45].

We can also utilize nanoscale synthesis techniques in the development of sensing materials, including methods like electrospinning and hydrothermal synthesis [65]. These approaches can yield a variety of innovative one-dimensional (1D) nanostructured sensing materials based on MOs [66]. Numerous studies have demonstrated the progression of non-biological analyte detection. These studies have explored various sensor types based on receptors and transducers, along with contemporary techniques utilizing nanomaterials like noble metal nanoparticles (NPs), nanocrystalline [67], MO NPs, nanowires (NWs) [68], nanorods (NRs),

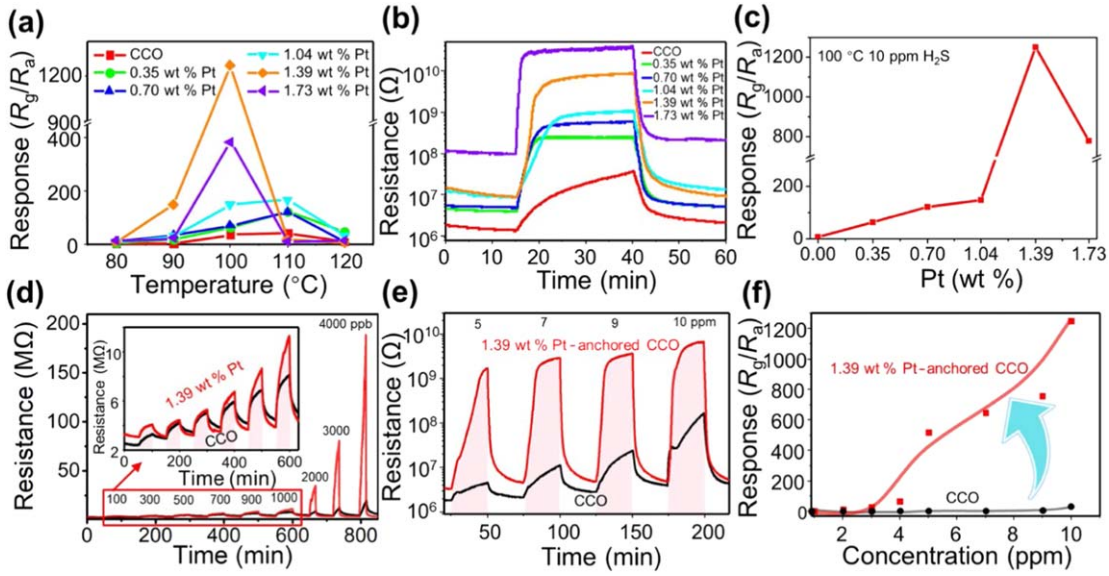

Figure 15. (a) Response of all chemiresistors to 10 ppm H_2S at 80 °C–120 °C. (b) Dynamic response curves to 10 ppm H_2S at 100 °C. (c) Response (to 10 ppm H_2S) vs Pt ratio at 100 °C. Successive response curves of pure and 1.39 wt% Pt-anchored CCO chemiresistors to (d) 100–4000 ppb and (e) 5–10 ppm H_2S at 100 °C. (f) Response of pure and 1.39 wt% Pt-anchored CCO chemiresistors vs H_2S concentration at an operating temperature of 100 °C [45] Copyright 2022, ACS.

carbon nanotubes (CNTs), quantum dots (QDs), and dendrimers. These advancements underscore the integration of nanotechnology into sensing technology. 1D nanomaterial-based sensors, commonly referred to as 1D nanosensors, offer several advantages compared to conventional bulk sensing materials. These advantages encompass enhanced sensitivity to target analytes, swifter response times, and reduced weight and power consumption. These benefits are chiefly attributed to the substantial augmentation of the surface area to volume ratio, heightened surface activity, and augmented charge carrier mobility achievable at the nanoscale. In the case of 1D nanomaterials featuring a limited density of defects, there tends to be a relatively minimal presence of crystalline boundaries that typically scatter charge carriers. Moreover, in the context of 1D materials boasting sufficiently diminutive diameters, charge carriers become constrained radially while retaining freedom of movement axially [69]. This dual characteristic synergistically fosters efficient charge carrier transportation. Furthermore, the potential for direct growth of 1D nanomaterials onto established microelectrodes brings forth the opportunity for seamless integration. This integration not only maintains low contact resistance between the sensing material and the electrode but also facilitates the scalability of nanosensors [70].

3.2. Advances in Technology

Achieving enhanced functionality and portability of sensors and their associated electronics is a significant challenge that requires miniaturization. Recent progress in nanoelectronics holds promise in addressing this challenge by enabling the development of smaller and more efficient sensors and electronics [71]. To meet the difficulties of modern healthcare systems, significant research has been dedicated to developing improved portable devices that utilize microelectromechanical systems (MEMS) and nanoelectromechanical systems (NEMS) for sensing and separating critical non-biological analytes. To achieve this goal, AI (artificial intelligence), advanced ML (machine learning) techniques and IoT (internet of Things) integration can be employed to develop highly selective and sensitive smart sensors.

ML techniques are increasingly being integrated into sensor development to enhance performance, accuracy, and efficiency. ML can help in various aspects of sensor operation such as data analysis and pattern recognition, sensor calibration, feature extraction, dynamic response prediction, fault detection and quality control, sensor array fusion, optimal material design, and adaptive sensing [73]. Incorporating ML in sensor development offers the potential to create smarter, more adaptable sensors with improved detection capabilities, reduced false alarms, and optimized performance across various applications. Using supervised learning algorithms like support vector machines (SVM), random forests, or neural networks to study the behaviour of the sensor responses [74]. Designing ML models that can provide real-time analysis of sensor data, enabling rapid detection and response to changes in analyte concentrations. In the present day, various researchers working on portable and self-powered systems utilizing piezoelectric and triboelectric nanogenerators exhibit the potential to partially address the aforementioned limitations. This approach can offer effective data

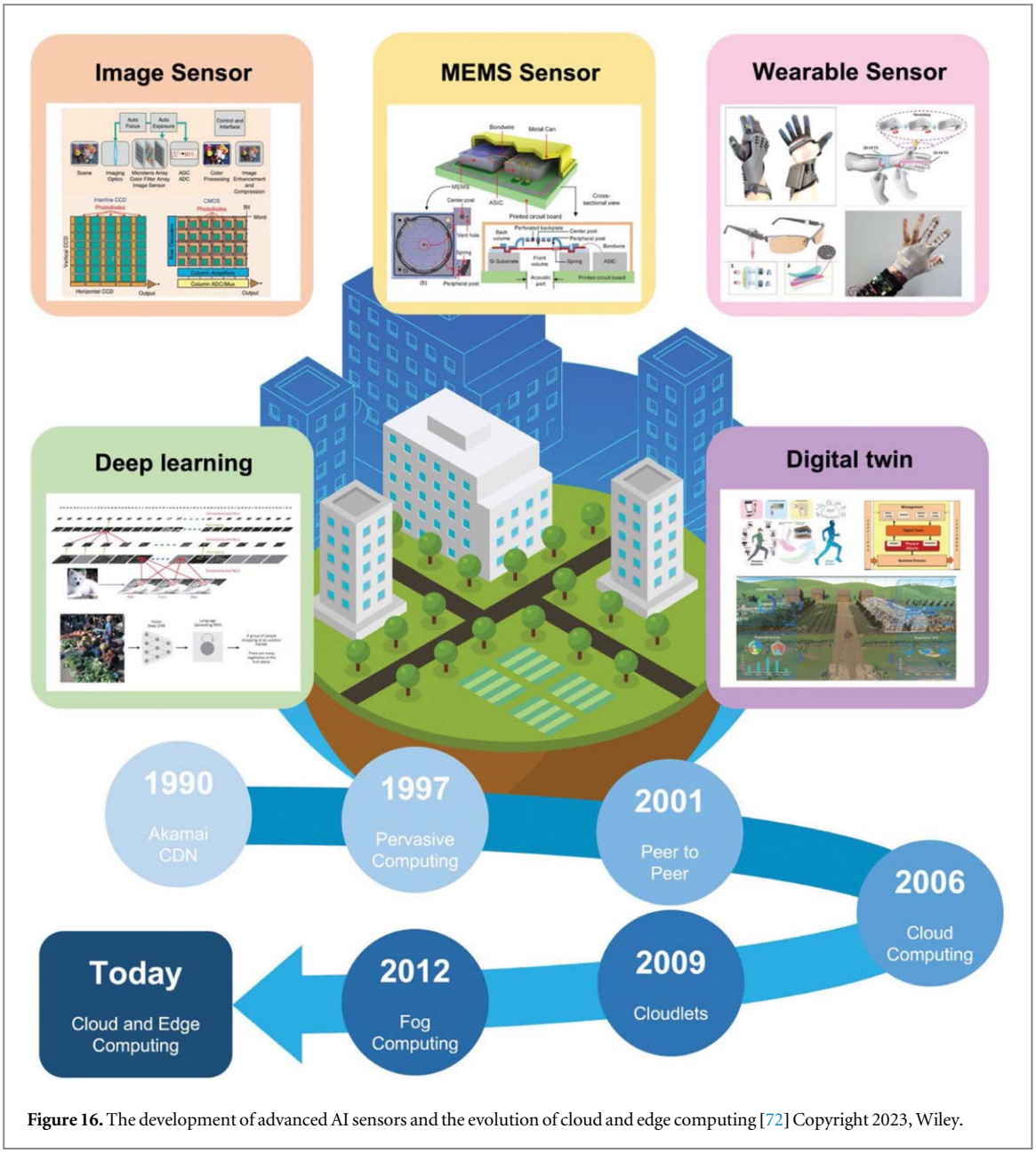

Figure 16. The development of advanced AI sensors and the evolution of cloud and edge computing [72] Copyright 2023, Wiley.

processing methods that enable the development of advanced sensing devices. By merging wearable sensors with AI data analytics, it becomes possible to capture signals associated with muscle deformation, joint flexion, temperature fluctuations, heartbeat frequency, and more. These data hold immense significance and find extensive use in domains like healthcare, environmental monitoring, human-machine interactions (HMI), and plant monitoring applications, as illustrated in figure 16 [72].

An array of sensors was affixed onto a printed circuit board and situated inside a sensing chamber with a capacity of 200 mL, illustrated in figure 17(a). Individual sensors were associated with alumina tubes encompassing heaters, which were soldered onto a Bakelite base. This sensor configuration is schematically depicted in figure 17(b). To construct a voltage divider circuit, the sensors were interlinked in series with predefined resistances, as illustrated in figure 17(c). On a personal computer, ML algorithms (figures 18(d)–(f)) were executed. Jin-Young Kim *et al* examined and resolved the issue of cross-sensitivity in MOs sensors by constructing a sensor array and then employing neural network-assisted pattern recognition analysis ML methods to analyze the data obtained from the array of sensors. To detect hazardous gases such as CO and NO_2, both individually and as mixtures, a compact array of metal oxide-based sensors was assembled. This array, featuring sensors constructed from Au-ZnO, Au-SnO_2, Pt-SnO_2, and unadorned In_2O_3, displayed the ability to selectively identify the specified gases even within complex environments, including various humid atmospheres. Utilizing this sensor array, it was possible to distinguish between binary mixtures containing different concentrations of CO and NO_2. This differentiation was achieved across 25 distinct CO-NO_2

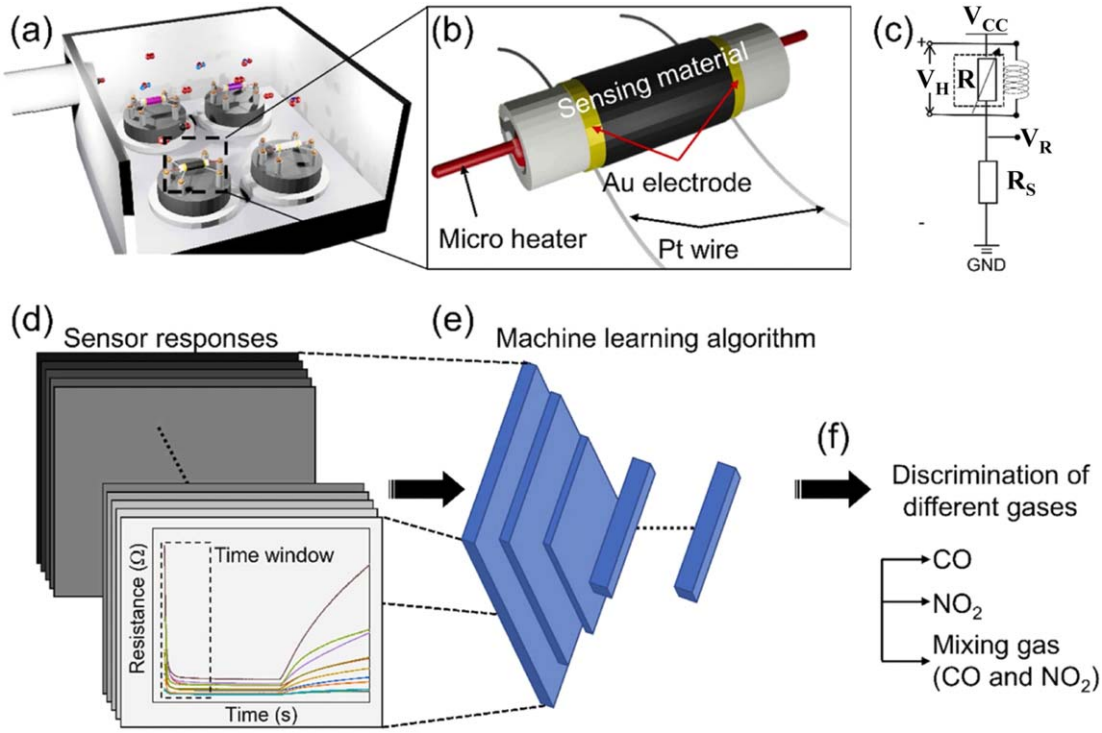

Figure 17. Schematics of a (a) gas sensor array, (b) fabricated gas sensor, (c) voltage divider circuit and heater connection, (d)–(f) ML-assisted classification and regression of CO and NO_2 and their mixtures [75] Copyright 2023, Elsevier.

concentration combinations in dry air and 13 such combinations in two atmospheres with differing levels of relative humidity. The array's capacity for effective discrimination was demonstrated using Principal Component Analysis (PCA), which employed response values for various gases and their amalgamations. Furthermore, a novel approach was devised to capture comprehensive response and recovery patterns as inputs. This strategy mitigates information loss arising from these patterns, ultimately enhancing the accuracy of gas detection processes. [75]. The precision achieved during the training phase is depicted in figure 18(a). After subjecting the adapted model to 500 iterations, employing the response values as inputs, it demonstrated a discrimination accuracy of 98.6%, as evidenced in figure 18(b). Notably, due to the significant reduction in data dimensions facilitated by PCA, the model selected for training with 500 epochs exhibited robust performance, attaining a flawless discrimination accuracy of 100%, as illustrated in figure 18(c). This robust performance can be attributed to the sensor array's capacity to generate high-quality fingerprints and the streamlined temporal information dimensionality. Consequently, the model achieved a perfect accuracy of 100%, as demonstrated in figure 18(d). Moreover, the researchers concluded that employing PCA on merely 25 and 10 data points and subsequently training these data with MLP-based models can yield accuracy exceeding 99.9%. This assertion is supported by the findings depicted in figures 18(e) and (f) respectively.

Radislav A Potyrailo *et al* that conventional semiconductor metal oxide materials have the potential to offer high-performance sensors using an impedance measurement method [76]. Their strategy involves utilizing dielectric excitation measurements and results in sensors characterized by a linear gas response (with R2 exceeding 0.99), a wide dynamic range for gas detection (encompassing six decades of concentrations), strong baseline stability, and diminished susceptibility to humidity and ambient temperature variations [76]. Impedance measurements of this kind can be applied for baseline correction, addressing a significant challenge associated with MOS-based sensors as shown in figures 19(a)–(e) at particular frequency its based line impedance almost remain constant. Considering this methodology is adaptable for implementation with both n-type and p-type MOs materials. Furthermore, this type of demonstration can be used in contexts such as wireless sensor networks, drone-based systems, and wearable devices for monitoring environmental and industrial gas levels.

Arnab Maity *et al* utilized a blend of wet transfer, impedance and noise assessments, along with ML techniques, to enable the large-scale production of sensor arrays based on graphene field-effect transistors (GFETs) [77]. Figures 20(a)–(l) illustrate the schematic experimental configuration for continuous sensing, along with the corresponding outcomes. This strategy effectively identified faulty devices. The sensors they developed demonstrated the capability to concurrently detect heavy-metal ions (lead and mercury) as well as

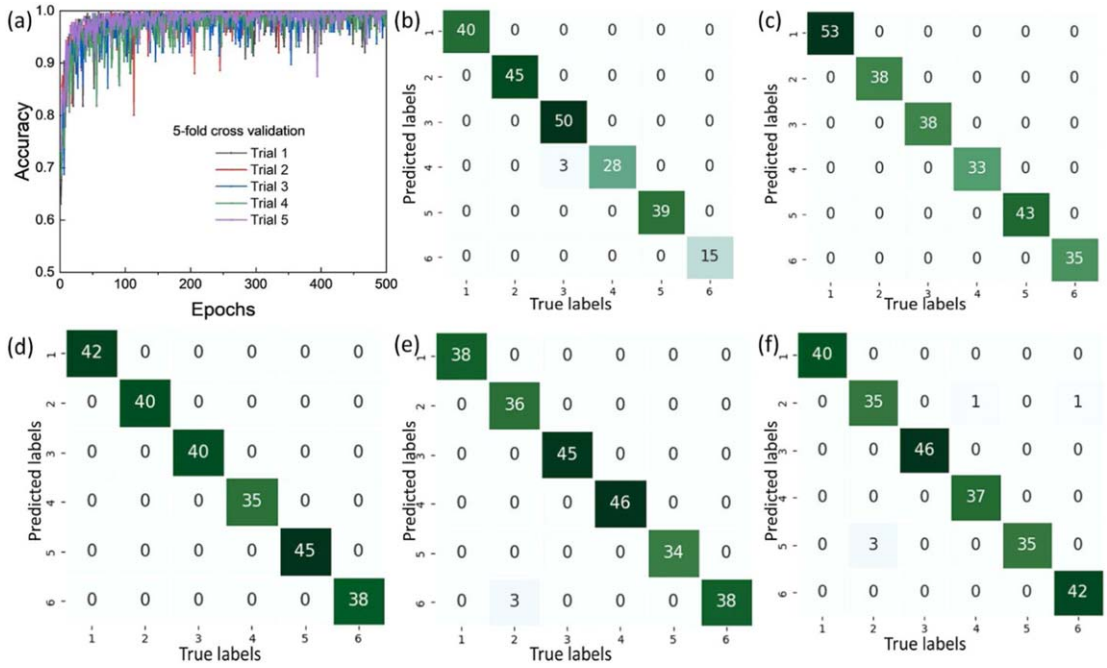

Figure 18. (a) Five-fold cross-validation accuracy of multilayer perceptron (MLP) with response values as input; (b) confusion matrix for predicting using response values; and confusion matrices for PCA-assisted MLP using (c) 400, (d) 200, (e) 25, and (f) 10 data points [75] Copyright 2023, Elsevier.

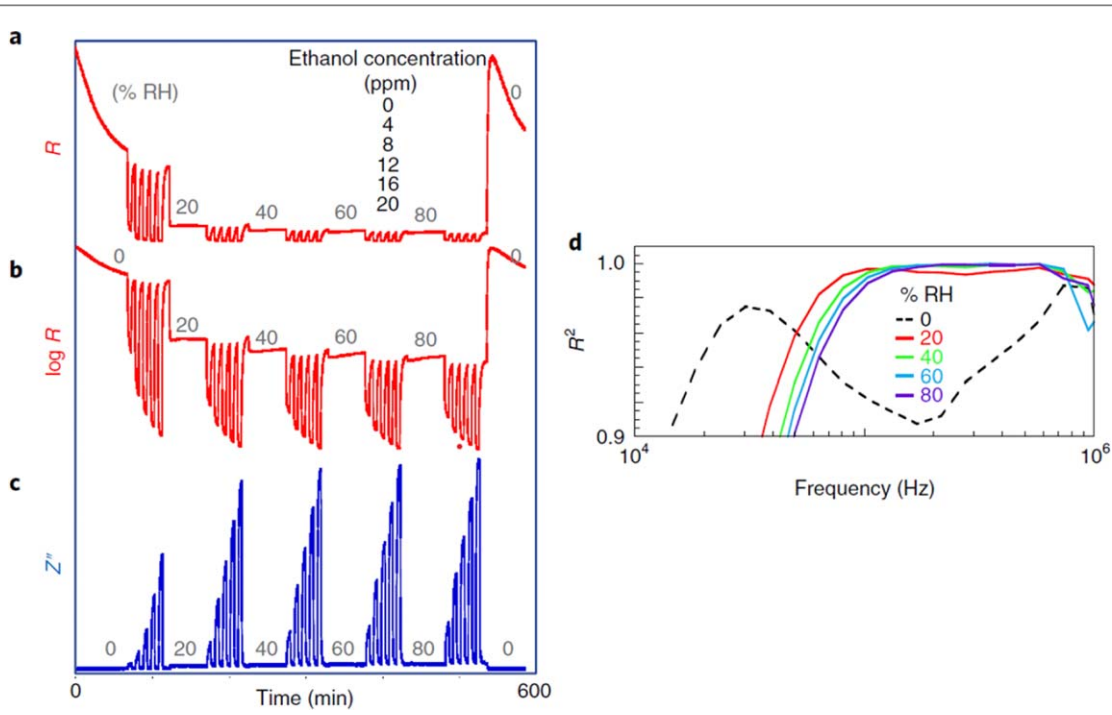

Figure 19. Effects of ambient humidity from 0 to 80% RH on exposures to ethanol vapour on the resistance response, linear scale (a), resistance response, (b) logarithmic scale (c) and dielectric response (Z'' at 0.17 MHz) with a dramatic reduction in the RH effects (d), and the frequency dependence of R^2 values of the linear fit for different RH levels [76]. Copyright 2020, Nature.

E. coli bacteria in real-time within a continuous flow of tap water [77]. Gehad Abd El-Fatah *et al* have introduced a technique called differential pulse voltammetry (DPV) that employs a composite electrode comprising gallium oxide nanoparticles and carbon paste (Ga_2O_3/CPE). This innovative approach enables the concurrent detection of Pb^{2+}, Cd^{2+}, and Hg^{2+} ions. The gallium oxide nanoparticles (Ga_2O_3 NPs) were synthesized using chemical

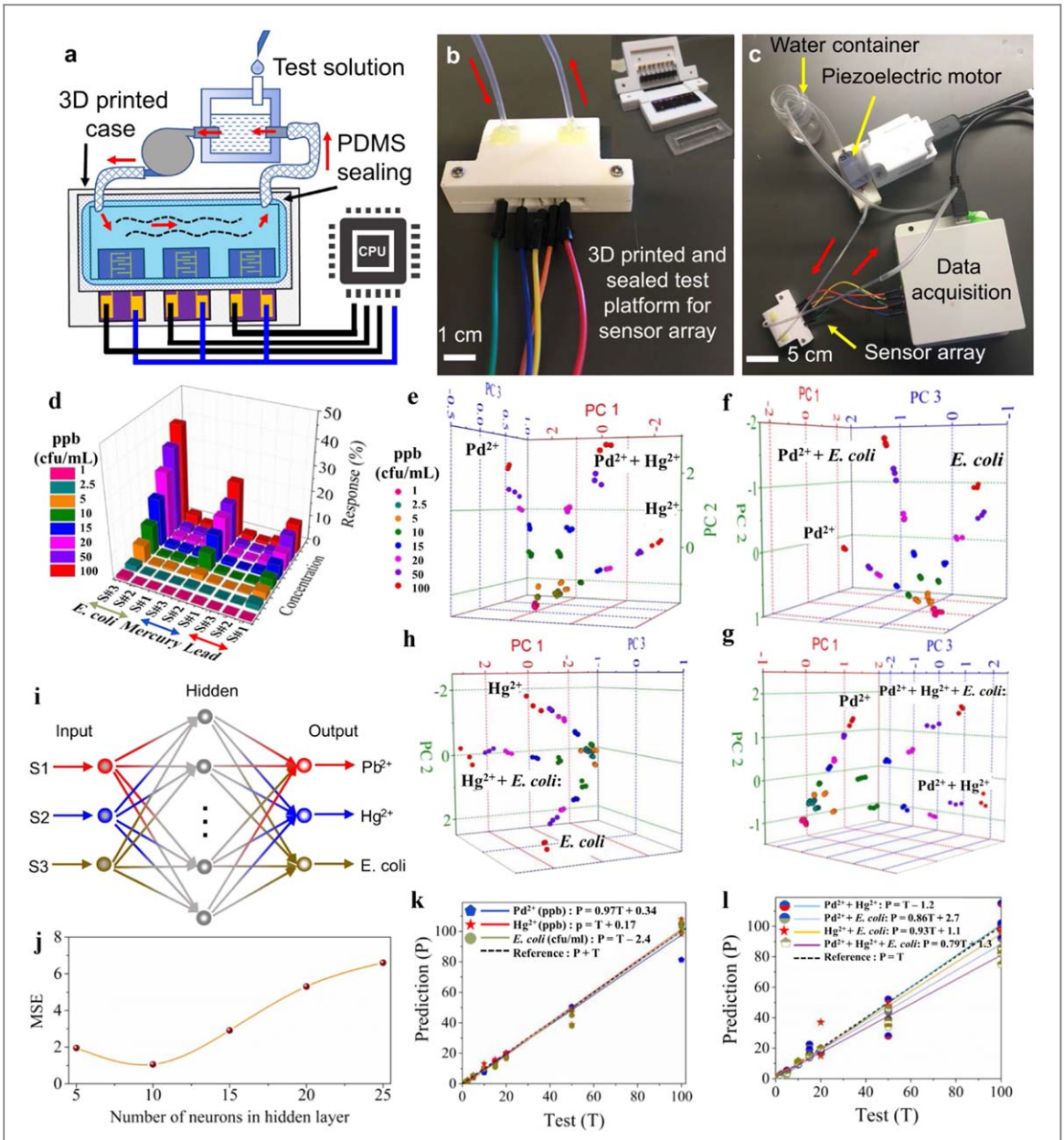

Figure 20. (a) Schematic experimental setup for continuous sensing. The sensor array housed in the chamber is sealed with a polydimethylsiloxane (PDMS) mold from the source-drain contact. Water is drawn by the piezoelectric motor into the sensor chamber and then continuously flows back to the external container to mimic the water flow. (b) Photograph of a 3D-printed sealed chamber with the sensors embedded inside. Inset is the cell interior. (c) Photograph of a piezoelectric micromotor and an external water container connected to the sealed sensor chamber. ML modelling for classifying and quantifying various mixed ionic and bacterial species in flowing water. (d) Summary of responses from Sensors 1-3 for Pb^{2+}, Hg^{2+}, and *E. coli*. (e–h) Principal component analysis (PCA) plots for the classifications of Pb^{2+}, Hg^{2+}, *E. coli*, and their mixtures. (i, j) Schematic of a two-layer artificial neural network (ANN) used for training and mean squared error (MSE) values for various numbers of neurons in the hidden layers. (k, l) Plots of the test and the predicted concentrations for Pb^{2+}, Hg^{2+}, and *E. coli* (ppb or cfu/mL) and their mixtures from the trained ANN model. Here, the dash line (Y = T) represents the perfect match between the test and the predicted concentrations for unknown samples while the solid line represents the fitting of the target concentrations predicted from the trained ANN model [77] Copyright 2023, Nature.

methods. They established a sensing platform exhibiting a wide dynamic linear range spanning from 0.3 to 80 μM, along with low detection limits (LODs) of 84 nM, 88 nM, and 130 nM for Pb^{2+}, Cd^{2+}, and Hg^{2+} ions, respectively. Correspondingly, the limit of quantification (LOQ) values was determined to be 280 nM, 320 nM, and 450 nM for the respective ions [78].

Min-Ho Seo *et al* pioneered a self-powered hydrogen (H_2) gas sensor employing a photovoltaic cell and a chemo-mechanically deformed Pd-PUA nanograting structure as shown in figure 21(a)–(c) [79]. This innovative sensor mechanism capitalizes on alterations in the optical transmittance of the nanograting structure, triggered by the expansion of Pd subsequent to its reaction with H_2 gas. The ensuing change in current output from the photovoltaic cell facilitates detection. Operating solely on ambient light, the sensor negates the need for external electrical power. This sensor exhibited remarkable performance, detecting H_2 gas concentrations as low

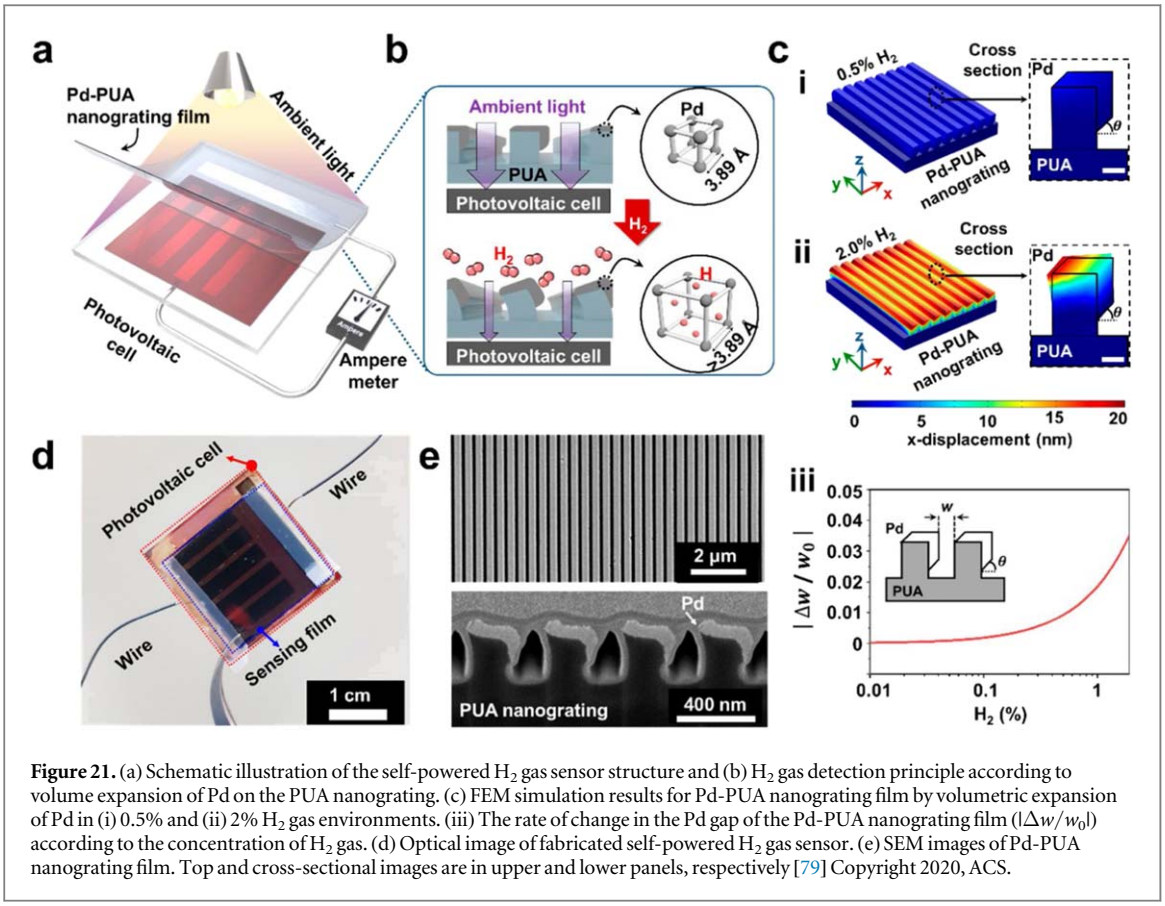

Figure 21. (a) Schematic illustration of the self-powered H_2 gas sensor structure and (b) H_2 gas detection principle according to volume expansion of Pd on the PUA nanograting. (c) FEM simulation results for Pd-PUA nanograting film by volumetric expansion of Pd in (i) 0.5% and (ii) 2% H_2 gas environments. (iii) The rate of change in the Pd gap of the Pd-PUA nanograting film ($|\Delta w/w_0|$) according to the concentration of H_2 gas. (d) Optical image of fabricated self-powered H_2 gas sensor. (e) SEM images of Pd-PUA nanograting film. Top and cross-sectional images are in upper and lower panels, respectively [79] Copyright 2020, ACS.

as 0.1%. It also showcased selectivity against CO, H_2S, and NO_2, along with substantial stability amidst humidity fluctuations. Its reliability, repeatability, and long-term viability reinforce its suitability for practical applications. Notably, the sensor's effectiveness persisted regardless of varying light intensities, enabling versatile deployment in settings where modest amounts of visible light are present. Furthermore, the research team seamlessly integrated the developed sensor into a portable H_2 gas leakage alarm system by coupling it with the Arduino platform and wireless communication as shown in figure 21(d), (e). This multifaceted achievement underscores the sensor's potential to revolutionize various contexts, including environmental monitoring and safety systems [79].

4. Concluding remarks

This review highlights an increasing numeral of publications focused on printed chemiresistive sensors, with a subsequent shift towards investigating fully digital-printed devices. Most non-biological analytes devices used in medical applications suffer large sample volumes, bringing about unreliable outcomes. Although there are a few exceptions such as electrochemical H_2O_2 sensors and lateral flow pregnancy tests, only a limited number of non-biological analytes have achieved widespread commercial success. Furthermore, there is a demand for affordable nanostructure-based analytes that can provide quick, accurate, and user-friendly results. To accomplish this, nanomaterials should be integrated into a tiny biochip (lab-on-chip) for efficient sample handling and multiplexed clinical diagnosis. Ongoing academic research in this field is expected to produce commercially viable prototypes soon. Notably, the research presented in wireless environmental and health monitoring has the potential to enrich daily life in the era of IoT, AI and ML. In the field of sensing researchers can more focus on portable and self-power sensors utilizing piezoelectric and triboelectric nanogenerators exhibit the potential to partially address the aforementioned limitations. However, the implementation of these technologies is complex, expensive, power-intensive, and requires a significant hardware setup to be deployed in real-world applications. Hence, it is recommended that novel materials be developed, and efficient data processing techniques utilizing ML algorithms be implemented to address issues related to selectivity and long-term stability in chemical non-biological analytes sensors. In the future, digital printing technology has the potential to enable the complete manufacturing of chemical systems, specifically chemiresistive sensor systems capable of simultaneously detecting various environmental changes. This approach would offer considerable savings in terms of materials, time, and costs when compared to conventional manufacturing and integration methods.

Enhanced comprehension and swift advancements in nanotechnology hold the potential to address the impending challenges that modern society will encounter.

Acknowledgments

The authors acknowledge the financial support of the Brain Pool Programme, Grant No.: 2022H1D3A2A01093549 by National Research Foundation of Korea.

Data availability statement

No new data were created or analysed in this study.

ORCID iDs

Sang Sub Kim https://orcid.org/0000-0001-6912-3509
Hyoun Woo Kim https://orcid.org/0000-0002-6118-9914
Mahesh Kumar https://orcid.org/0000-0002-5357-7300

References

[1] Elanjeitsenni V P, Vadivu K S and Prasanth B M 2022 A review on thin films, conducting polymers as sensor devices *Mater. Res. Express* **9** 022001
[2] Liu F, Gillan L, Leppäniemi J and Alastalo A 2023 Focused review on print-patterned contact electrodes for metal-oxide thin-film transistors *Adv. Mater. Interfaces* **10** 2202258
[3] Wang X *et al* 2020 Large-area flexible printed thin-film transistors with semiconducting single-walled carbon nanotubes for NO_2 sensors, *ACS Appl. Mater. Interfaces* **12** 51797–807
[4] Tehrani Z *et al* 2020 Printable and flexible graphene pH sensors utilising thin film melanin for physiological applications *2D Mater.* **7** 024008
[5] Song O *et al* 2022 All inkjet-printed electronics based on electrochemically exfoliated two-dimensional metal, semiconductor, and dielectric *npj 2D Mater. Appl.* **6** 64
[6] Chen Y, Li M, Yan W, Zhuang X, Ng K W and Cheng X 2021 Sensitive and low-power metal oxide gas sensors with a low-cost microelectromechanical heater *ACS Omega* **6** 1216–22
[7] Kaur N, Singh M and Comini E 2022 Materials engineering strategies to control metal oxides nanowires sensing properties *Adv. Mater. Interfaces* **9** 2101629
[8] Wieszczycka K, Staszak K, Woźniak-Budych M J, Litowczenko J, Maciejewska B M and Jurga S 2021 Surface functionalization—The way for advanced applications of smart materials, *Coord. Chem. Rev.* **436** 213846
[9] Fadeel B *et al* 2018 Safety assessment of graphene-based materials: focus on human health and the environment *ACS Nano* **12** 10582–620
[10] Jin L, Griffith S M, Sun Z, Yu J Z and Chan W 2021 On the flip side of mask wearing: increased exposure to volatile organic compounds and a risk-reducing solution *Environ. Sci. Technol.* **55** 14095–104
[11] Wang W *et al* 2022 Internal exposure and distribution of airborne fine particles in the human body: methodology, current understandings, and research needs *Environ. Sci. Technol.* **56** 6857–69
[12] Mitra S *et al* 2022 Impact of heavy metals on the environment and human health: novel therapeutic insights to counter the toxicity *J. King Saud Univ. - Sci.* **34** 101865
[13] Naidu R *et al* 2021 Chemical pollution: a growing peril and potential catastrophic risk to humanity *Environ. Int.* **156** 106616
[14] Shaik R, Kampara R K, Kumar A, Sharma C S and Kumar M 2022 Metal oxide nanofibers based chemiresistive H_2S gas sensors, *Coord. Chem. Rev.* **471** 214752
[15] Radha K, Selvaraj B, Srinivasan P, Krishnakumar A, Rayappan J B B and Babu K J 2021 Room-temperature acetaldehyde-sensing properties of SILAR-deposited ZnO thin films: role of tungsten doping *J. Mater. Sci., Mater. Electron.* **32** 17700–15
[16] Tripathy N and Kim D H 2018 Metal oxide modified ZnO nanomaterials for biosensor applications *Nano Converg.* **5** 1–10
[17] Sukanya R, Ramki S, Chen S M and Karthik R 2020 Ultrasound treated cerium oxide/tin oxide (CeO2/SnO2) nanocatalyst: a feasible approach and enhanced electrode material for sensing of anti-inflammatory drug 5-aminosalicylic acid in biological samples *Anal. Chim. Acta* **1096** 76–88
[18] Azizah N *et al* 2016 Integrated titanium dioxide (TiO_2) nanoparticles on interdigitated device electrodes (IDEs) for pH analysis *AIP Conf. Proc.* **1733** 2–7
[19] Shanbhag M M, Shetti N P, Kalanur S S, Pollet B G, Nadagouda M N and Aminabhavi T M 2022 Hafnium doped tungsten oxide intercalated carbon matrix for electrochemical detection of perfluorooctanoic acid *Chem. Eng. J.* **434** 134700
[20] Verma D, Yadav A K, Mukherjee M D and Solanki P R 2021 Fabrication of a sensitive electrochemical sensor platform using reduced graphene oxide-molybdenum trioxide nanocomposite for BPA detection: an endocrine disruptor *J. Environ. Chem. Eng.* **9** 105504
[21] Xu J, Liu C and Teng Y 2010 Direct electrochemistry and electrocatalysis of hydrogen peroxide using hemoglobin immobilized in hollow zirconium dioxide spheres and sodium alginate films *Microchimica Acta* **169** 181
[22] Wang Y *et al* 2015 A novel electrochemical sensor based on zirconia / ordered macroporous polyaniline for ultrasensitive detection of pesticides *Analyst* **140** 560–6
[23] Maier D, Laubender E, Basavanna A, Schumann S, Urban G A and Dincer C 2019 Toward continuous monitoring of breath biochemistry: a paper-based wearable sensor for real-time hydrogen peroxide measurement in simulated breath *ACS sensors* **4** 2945–51
[24] Yang L, Qin M, Zhang G, Yang J, Yang J and Zhao J 2023 Progress of sensitive materials in chemiresistive sensors for detecting chemical warfare agent simulants: A review *Rev. Anal. Chem* **42** 20220052

[25] Lee J E, Lim C K, Park H J, Song H, Choi S Y and Lee D S 2020 ZnO-CuO core-hollow cube nanostructures for highly sensitive acetone gas sensors at the ppb level *ACS Appl. Mater. Interfaces* **12** 35688–97

[26] Dhahri R *et al* 2017 Enhanced performance of novel calcium/aluminum co-doped zinc oxide for CO_2 sensors, *Sensors Actuators, B Chem.* **239** 36–44

[27] Ahmad R, Ahn M S and Hahn Y B 2017 ZnO nanorods array based field-effect transistor biosensor for phosphate detection *J. Colloid Interface Sci.* **498** 292–7

[28] Wei Y *et al* 2012 SnO2/reduced graphene oxide nanocomposite for the simultaneous electrochemical detection of cadmium(II), lead (II), copper(II), and mercury(II): An interesting favorable mutual interference *J. phys. chem. C* **116** 1034–41

[29] Gao C, Yu X Y, Xiong S Q, Liu J H and Huang X J 2013 Electrochemical detection of arsenic(III) completely free from noble metal: Fe_3O_4 microspheres-room temperature ionic liquid composite showing better performance than gold *Anal. Chem.* **85** 2673–80

[30] Kulkarni P *et al* 2023 Morphological alterations in WO_3-SnO_2 heterostructures and their effects on chlorine sensing, *Sensors Actuators B Chem.* **388** 133800

[31] Jo Y K, Jeong S Y, Moon Y K, Jo Y M, Yoon J W and Lee J H 2021 Exclusive and ultrasensitive detection of formaldehyde at room temperature using a flexible and monolithic chemiresistive sensor *Nat. Commun.* **12** 4955

[32] Wang L, Zhang R, Zhou T, Lou Z, Deng J and Zhang T 2016 Concave Cu_2O octahedral nanoparticles as an advanced sensing material for benzene (C_6H_6) and nitrogen dioxide (NO_2) detection, *Sensors Actuators, B Chem.* **223** 311–7

[33] Kumar A, Shringi A K and Kumar M 2022 RF sputtered CuO anchored SnO_2 for H_2S gas sensor, *Sensors Actuators B Chem.* **370** 132417

[34] Alali K T *et al* 2020 HFIP-functionalized electrospun WO_3 hollow nanofibers/rGO as an efficient double layer sensing material for dimethyl methylphosphonate gas under UV-Light irradiation, *J. Alloys Compd.* **832** 1–12

[35] Cao P *et al* 2019 Ethanol sensing behavior of Pd-nanoparticles decorated ZnO-nanorod based chemiresistive gas sensors *Sensors Actuators, B Chem.* **298** 126850

[36] Wu K, He X, Ly A, Lahem D, Debliquy M and Zhang C 2023 Highly sensitive and selective gas sensors based on 2D/3D Bi_2MoO_6 micro-nano composites for trimethylamine biomarker detection, *Appl. Surf. Sci.* **629** 157443

[37] Majhi S M, Navale S T, Mirzaei A, Kim H W and Kim S S 2023 Strategies to boost chemiresistive sensing performance of In_2O_3-based gas sensors: an overview, *Inorg. Chem. Front.* **10** 3428–67

[38] Ferrag C and Kerman K 2020 Grand challenges in nanomaterial-based electrochemical sensors *Frontiers in Sensors* **1** 583822

[39] Sun C, Su X, Xiao F, Niu C and Wang J 2011 Synthesis of nearly monodisperse Co3O4 nanocubes via a microwave-assisted solvothermal process and their gas sensing properties *Sensors Actuators B. Chem.* **157** 681–5

[40] Shen S F, Xu M L, Lin D B and Pan H B 2017 The growth of urchin-like Co_3O_4 directly on sensor substrate and its gas sensing properties. *Appl. Surf. Sci.* **396** 327–32

[41] Wen Z, Zhu L, Mei W, Hu L, Li Y, Sun L, Cai H and Ye Z 2013 Rhombus-shaped Co_3O_4 nanorod arrays for high-performance gas sensor *Sensors Actuators* B **186** 172–9

[42] Suh J M, Shim Y S, Kwon K C, Jeon J M, Lee T H, Shokouhimehr M and Jang H W 2019 Pd-and Au-decorated MoS_2 gas sensors for enhanced selectivity *Electron. Mater. Lett.* **15** 368–76

[43] Singh S and Sharma S 2022 Temperature dependent selective detection of ethanol and methanol using MoS_2/TiO_2 composite *Sensors and Actuators B: Chemical* **350** 130798

[44] Lee K *et al* 2019 Highly selective reduced graphene oxide (rGO) sensor based on a peptide aptamer receptor for detecting explosives *Sci. Rep.* **9** 10297

[45] Zhang R *et al* 2022 Pt-anchored CuCrO2 for low-temperature-operating high- performance H2S chemiresistors *ACS Appl. Mater. Interfaces* **14** 24536–45

[46] Ahmad T, Phul R, Alam P, Lone I H, Shahazad M, Ahmed J, Ahamad T and Alshehri S M 2017 Dielectric, optical and enhanced photocatalytic properties of $CuCrO_2$ nanoparticles *RSC Adv.* **7** 27549–57

[47] Ganesamurthi J *et al* 2022 NiO/ZnO binary metal oxide based electrochemical sensor for the evaluation of hazardous flavonoid in biological and vegetable samples *Colloids Surfaces A Physicochem. Eng. Asp.* **647** 129077

[48] Krishna M S *et al* 2022 A review on 2D-ZnO nanostructure based biosensors: from materials to devices *Mater. Adv.* **4** 320–54

[49] Malode S J, Prabhu K, Kalanur S S, Meghani N and Shetti N P 2023 WO_3/rGO nanocomposite-based sensor for the detection and degradation of 4-Chlorophenol, *Chemosphere* **312** 137302

[50] Chen Y, Liu B, Chen Z and Zuo X 2021 Innovative electrochemical sensor using TiO_2 nanomaterials to detect phosphopeptides *Anal. Chem.* **93** 10635–43

[51] Ameen S, Kim E B, Akhtar M S and Shin H S 2017 Electrochemical detection of resorcinol chemical using unique cabbage like ZnO nanostructures *Mater. Lett.* **209** 571–5

[52] Joshi N, Hayasaka T, Liu Y, Liu H, Oliveira O N and Lin L 2018 A review on chemiresistive room temperature gas sensors based on metal oxide nanostructures, graphene and 2D transition metal dichalcogenides *Microchim. Acta* **185** 1–16

[53] Luo M, Fan T, Zhou Y, Zhang H and Mei L 2019 2D black phosphorus–based biomedical applications *Adv. Funct. Mater.* **29** 1808306

[54] Riazi H, Nemani S K, Grady M C, Anasori B and Soroush M 2021 Ti_3C_2 MXene–polymer nanocomposites and their applications *J. Mater. Chem.* A **9** 8051–98

[55] Noremberg B S *et al* 2017 From banana stem to conductive paper: a capacitive electrode and gas sensor *Sensors Actuators, B Chem.* **240** 459–67

[56] Zhu L Y, Ou L X, Mao L W, Wu X Y, Liu Y P and Lu H L 2023 Advances in Noble Metal-Decorated Metal Oxide Nanomaterials for Chemiresistive Gas Sensors: Overview *Nano-Micro Letters* **15** 89

[57] Goel N, Kunal K, Kushwaha A and Kumar M 2023 Metal oxide semiconductors for gas sensing *Engineering Reports* **5** e12604

[58] Yoon Y, Truong P L, Lee D and Ko S H 2022 Metal-oxide nanomaterials synthesis and applications in flexible and wearable sensors *ACS Nanosci. Au* **2** 64–92

[59] Mondal B and Gogoi P K 2022 Nanoscale heterostructured materials based on metal oxides for a chemiresistive gas sensor *ACS Appl. Electron. Mater.* **4** 59–86

[60] Singh A, Sikarwar S, Verma A and Yadav B C 2021 The recent development of metal oxide heterostructures based gas sensor, their future opportunities and challenges_ a review *Sensors and Actuators A: Physical* **332** 113127

[61] Ali J, Najeeb J, Ali M A, Aslam M F and Raza A 2017 Biosensors: their fundamentals, designs, types and most recent impactful applications: a review *J. Biosens. Bioelectron* **8** 1–9

[62] Zhao M, Yu J, Zhang X, Li Z, Ding Y and Edel J B 2021 Tuning interfacial energy barriers in heterojunctions for anti-interference sensing *Advanced Functional Materials* **31** 2008604

[63] Zubiarrain-Laserna A, Angizi S, Akbar M A, Divigalpitiya R, Selvaganapathy P R and Kruse P 2022 Detection of free chlorine in water using graphene-like carbon based chemiresistive sensors *RSC advances* **12** 2485–96

[64] Choi P G, Fuchigami T, Kakimoto K and Masuda Y 2020 Effect of crystal defect on gas sensing properties of Co3O4 nanoparticles *ACS Sensors* **5** 1665–73
[65] Chen L *et al* 2022 Chemiresistive gas sensors based on electrospun semiconductor metal oxides: A review *Talanta* **246** 123527
[66] Yang B, Myung N V and Tran T 2021 1D metal oxide semiconductor materials for chemiresistive gas sensors: a review *Advanced Electronic Materials* **2100271** 1–37
[67] Shah A Y, Choudhury S and Betty C A 2023 Reliable liquified petroleum gas sensing at room temperature by nanocrystalline SnO_2 thin film deposited by Langmuir–Blodgett method, *Appl. Phys. A Mater. Sci. Process.* **129** 1–10
[68] Shah V, Bhaliya J, Patel G M and Joshi P 2022 Room-temperature chemiresistive gas sensing of SnO2 nanowires: a review *Journal of Inorganic and Organometallic Polymers and Materials* **32** 741–72
[69] Adamu B I, Chen P and Chu W 2021 Role of nanostructuring of sensing materials in performance of electrical gas sensors by combining with extra strategies *Nano Express* **2** 042003
[70] Electrocatalysts W, Li J and Zheng G 2017 One-dimensional earth-abundant nanomaterials for water-splitting electrocatalysts *Advanced Science* **4** 1600380
[71] Arakawa T, Dao D V and Mitsubayashi K 2022 Biosensors and chemical sensors for healthcare monitoring: a review *IEEJ Trans. Electr. Electron. Eng.* **17** 626–36
[72] Zhang Z, Wang L and Lee C 2023 Recent Advances in Artificial Intelligence Sensors *Advanced Sensor Research* **2** 2200072
[73] Soori M, Arezoo B and Dastres R 2023 Artificial intelligence, machine learning and deep learning in advanced robotics, a review *Cogn. Robot.* **3** 54–70
[74] Ballard Z, Brown C, Madni A M and Ozcan A 2021 Machine learning and computation-enabled intelligent sensor design *Nat. Mach. Intell.* **3** 556–65
[75] Kim J Y, Bharath S P, Mirzaei A, Kim H W and Kim S S 2023 Classification and concentration estimation of CO and NO_2 mixtures under humidity using neural network-assisted pattern recognition analysis, *J. Hazard. Mater.* **459** 132153
[76] Potyrailo R A *et al* 2020 Extraordinary performance of semiconducting metal oxide gas sensors using dielectric excitation *Nat. Electron.* **3** 280–9
[77] Maity A *et al* 2023 Scalable graphene sensor array for real-time toxins monitoring in flowing water *Nat. Commun.* **11** 4184
[78] El-Fatah G A, Magar H S, Hassan R Y A, Mahmoud R, Farghali A A and Hassouna M E M 2022 A novel gallium oxide nanoparticles-based sensor for the simultaneous electrochemical detection of Pb^{2+}, Cd^{2+} and Hg^{2+} ions in real water samples, *Sci. Rep.* **12** 1–14
[79] Seo M H *et al* 2020 Chemo-mechanically operating palladium-polymer nanograting film for a self-powered H_2gas sensor *ACS Nano* **14** 16813–22